Inhibition of PDE4/PDE4B improves renal function and ameliorates inflammation in cisplatin-induced acute kidney injury

Man Xu[1,2,4*], Xiaowen Yu[1,3,4*], Xia Meng[1,3,4], Songming Huang[1,3,4], Yue Zhang[1,3,4], Aihua Zhang[1,3,4], and Zhanjun Jia[1,3,4]

[1] Department of Nephrology, Children's Hospital of Nanjing Medical University, Gulou District, Guangzhou Road #72, Nanjing 210008, China

[2] Department of Endocrinology, Children's Hospital of Nanjing Medical University, Gulou District, Guangzhou Road #72, Nanjing 210008, China

[3] Jiangsu Key Laboratory of Pediatrics, Nanjing Medical University, Gulou Distric, Hanzhong Road #140, Nanjing 210029, China

[4] Nanjing Key Laboratory of Pediatrics, Children's Hospital of Nanjing Medical University, Gulou District, Guangzhou Road #72, Nanjing 210008, China

*Man Xu and Xiaowen Yu equally contributed to this work

Correspondence to:

Zhanjun Jia, Department of Nephrology, Children's Hospital of Nanjing Medical University, Gulou District, Guangzhou Road #72, Nanjing 210008, China, Tel: 0086-25-8311-7309, Fax: 0086-25-8330-4239, Email: jiazj72@hotmail.com.

Running Title: PDE4/PDE4B in AKI

ABSTRACT

Nephrotoxicity is a known clinical complication of cisplatin that limits the use of this potent antitumour drug. Cyclic nucleotide phosphodiesterases (PDEs) play complex roles in physiology and pathology. PDE4, which is a member of the PDE family, has four subtypes (PDE4A-D), and PDE4B plays an important role in inflammation. Thus, in the present study, we investigated the effect of PDE4/PDE4B inhibition on renal function and inflammation in a cisplatin nephrotoxicity model. In mice, cisplatin enhanced the mRNA and protein expression of PDE4B in the renal tubules. After treatment with the PDE4 inhibitor cilomilast, cisplatin-induced renal dysfunction, renal tubular injury, tubular cell apoptosis, and inflammation were all improved. Next, after silencing PDE4B in vivo, we observed a protective effect against cisplatin nephrotoxicity similar to that of the PDE4 inhibitor. In vitro, cisplatin-induced renal tubular cell death was strikingly ameliorated by the PDE4 inhibitor and PDE4B knockdown along with the blockade of the inflammatory response. Considering the known roles of some cell survival pathways in antagonizing insults, we examined the levels of the PDE4-associated proteins Sirt1, PI3K, and phosphorylated AKT in cisplatin-treated renal tubular cells with or without cilomilast treatment. Strikingly, cisplatin treatment downregulated the expression of the above proteins, and this effect was largely abolished by the PDE4 inhibitor. Together, these findings indicate the beneficial role of PDE4/PDE4B inhibition in treating cisplatin nephrotoxicity, possibly through antagonizing inflammation and restoring cell survival signalling pathways.

Key words: PDE4, PDE4B, cilomilast, cisplatin, acute kidney injury

INTRODUCTION

Cisplatin is a widely used chemotherapeutic agent for treating solid tumors. However, the application of cisplatin has many side effects, including nephrotoxicity, ototoxicity, nausea and vomiting, and neurotoxicity. Nephrotoxicity occurs in approximately one-third of patients after a single dose of therapy of cisplatin (50-100 mg/m^2), and nephrotoxicity can result in acute kidney injury (AKI), which is characterized by high morbidity and high mortality(25, 26) . A large number of studies have confirmed that AKI is an important risk factor for the occurrence and progression of chronic kidney disease (CKD)(2) . Currently, there is no satisfactory treatment for AKI, including cisplatin nephrotoxicity.

Cyclic adenosine monophosphate (cAMP) is an important second signaling molecule in cells. The balance of intracellular cAMP levels is mainly dependent on two enzymes: Adenyl cyclase (AC), which plays a major role in cAMP synthesis and cyclic nucleotide phosphodiesterases (PDEs), which mainly function in hydrolysis (33). In mammals, PDEs can be divided into 11 families, namely, PDE1-PDE11(35) . Among them, PDE4 hydrolyses cAMP specifically. PDE4 has four subtypes, namely, PDE4A, PDE4B, PDE4C, and PDE4D, which are encoded by four independent genes: A, B, C, and D (11) .

Studies have confirmed that the inhibition of PDE4 can inhibit multiple inflammatory responses in vitro and in vivo. PDE4 inhibitors have been developed

and confirmed to be having anti-inflammatory effects in various animal models of diseases, including asthma, chronic obstructive pulmonary disease (COPD), psoriasis, inflammatory bowel disease and rheumatoid arthritis(36) . Some PDE4 inhibitors have been tested in clinical trials for asthma and COPD (5, 21, 37) .

Some researchers have suggested that PDE4B, which is also the major PDE4 subtype in monocytes and neutrophils, but not other subunits, plays a major role in triggering inflammation(39) , and non-selective inhibitors of PDE4B are commonly used to interfere with inflammatory lung disease (8) . Gene knockout experiments have shown that the knockdown of PDE4B reduces LPS-induced TNF-α expression, but knocking out PDE4D does not affect TNF-α expression (14) , suggesting that PDE4B may be more important than other subtypes of PDE4 in the process of inflammation. PDE4 inhibitors can improve kidney damage by increasing cAMP expression after renal ischemia-reperfusion injury in rats (23) . In mouse unilateral ureteral obstruction (UUO) models, PDE4 inhibitors can reduce renal interstitial fibrosis and TGF-β1-induced RTEC (renal tubular epithelial cells) damage in vitro(6). However, the role of PDE4/PDE4B in cisplatin-induced AKI is still unclear, and whether its inhibitors can improve cisplatin-induced renal damage remains to be further explored.

In this study, a PDE4 inhibitor and PDE4B silencing were used to investigate the roles of PDE4/PDE4B on cisplatin nephrotoxicity in both mouse and cell models.

MATERIAL AND METHODS

Chemicals and kits. Cilomilast (N98% pure) was purchased from Selleck. Dulbecco's modified Eagle's medium (DMEM), foetal bovine serum (FBS), and trypsin solution (EDTA) were purchased from Gibco (Invitrogen, Grand Island, NY). Antibodies against PDE4A (Cat.No.16226-1-AP), PDE4C (Cat.No.21754-1-AP), PDE4D (Cat.No.12918-1-AP) and PI3K (Cat.No.20584-1-Ig) were provided by Protein Tech (Chicago, IL, USA). Antibodies against BAX (Cat.No.14796), caspase-3 (Cat.No.9662), cleaved caspase-3 (Cat.No.9664), Sirt1 (Cat.No.8469), AKT (Cat.No.4685), phospho-AKT (pAKT) (Cat.No.4060) and GAPDH (Cat.No.3683), were all from Cell Signaling Technology (Danvers, MA, USA). Antibodies against NGAL (Cat.No.ab63929) and PDE4B (Cat.No.ab14611) (22) were purchased from Abcam (Cambridge, MA, USA). A horseradish peroxidase (HRP)- conjugated goat anti-rabbit secondary antibody was also obtained from Cell Signaling Technology (Danvers, MA, USA).

Experimental animals. Adult male C57BL/6 mice (6-8 weeks old) were purchased from the Mode Animal Research Center of Nanjing University (Nanjing, China) and used for our studies. The animals were housed at the animal facilities of the Experimental Animal Center of Nanjing Medical University with free access to food and water and under a 12 h light-dark cycle (lights on at 6:00 a.m. and lights off at 6:00 p.m.). All animal procedures were approved by the Nanjing Medical University Institutional Animal Care and Use Committee (registration number: IACUC1809017). We administered 2 different treatments. First, we pretreated mice with cilomilast (30

mg/kg) by i.p. injection for 24 h and then administered a single i.p. injection of cisplatin (20 mg/kg). Cilomilast was continuously administered for the next 3 days until the animals were sacrificed (after cisplatin injection for 3 days). Second, we designed short hairpin RNAs (sequence: TGACACCTTTGTAACCTACATGATGACTTTAGAAGACCATT) to silence PDE4B (shPDE4B) with empty vectors as negative control (NC). 60 μg of shPDE4B or NC plasmids was administered to mice within 10 s via tail vein injection. After 36 h, cisplatin was administered as described above. All mice were sacrificed 72 h after cisplatin injection. The blood was collected, and the isolated serum was stored at -80°C. Kidney tissues for histological analysis were fixed in 4% paraformaldehyde (PFA). The remaining kidney tissues were stored at -80°C for mRNA and protein analysis.

Measurement of serum creatinine and blood urea nitrogen. Thirty-six hours after cisplatin injection, blood was collected from the inferior vena cava and centrifuged at 3000 rpm for serum collection. The levels of serum creatinine (SCr) and blood urea nitrogen (BUN) were determined using a serum biochemical autoanalyzer (Hitachi 7600 modular chemistry analyzer, Hitachi Ltd., USA).

Periodic acid-Schiff staining. The fresh kidneys were removed and fixed with 4% paraformaldehyde at room temperature for 24 h and then embedded in paraffin. The tissues were sliced into 3-μm sections, stained with periodic acid-Schiff (PAS) and examined by light microscopy. The pathological parameters used for the tubular injury scoring included tubular dilatation, cast formation, brush border loss, and

tubular cell necrosis. A minimum of 10 fields from each kidney slide were examined and scored for pathological injury. Degree of injury was graded on a scale from 0 to 4: 0, normal; 1, mild injury, <25% damage; 2, moderate injury, 25–50% damage; 3, severe injury, 50–75% damage; and 4, almost all tubules in field of view were damaged, >75% damage.

Immunohistochemistry. Paraffin-embedded kidney sections (3 μm) were stained with PDE4B (1:100) to observe localization and expression. Briefly, the sections were deparaffinized, and hydrated, and the endogenous peroxidase activity was inactivated by 5% H_2O_2. The sections were further blocked with blocking solution (Beyotime, Hangzhou, China) for 1h at room temperature following antigen retrieval and were then incubated with a rabbit monoclonal primary antibody PDE4B overnight at 4°C.The next day, the sections were washed 3 times with PBS. Then ENV (Dako, K5007) was added to each section and incubated for 30 min at 37°C. PDE4B was visualized with DAB (Dako, K5007). The sections were stained with haematoxylin to show the nucleus and were dehydrated and mounted with neutral balsam. Images were obtained using an Olympus BX51 microscope (Olympus, Center Valley, PA), and the signals were analysed using Image-Pro Plus software analysis tools.

TUNEL Assay. TUNEL assays were performed on paraffin-embedded tissue sections with an in situ apoptosis detection kit according to the manufacturer's instructions (Vazyme). Green fluorescence was detected by fluorescence microscopy identify apoptotic cells.

Cell culture and treatment. Mouse renal tubule epithelial cells (RTECs) were

obtained from the American Type Culture Collection (ATCC, Manassas, VA). The cells were cultured in DMEM/F-12 (Wisent, Canada) supplemented with 10% foetal bovine serum (Gibco), penicillin (100 U/mL) and streptomycin (100 μg/mL) and maintained at 37 °C in 5% CO_2 in a humidified incubator. The cells were grown to 80% confluence and pretreated with cilomilast for 40 min. Then, cisplatin (5 μg/mL) was added to the serum-free medium to stimulate the RTECs for 24 h. The RTECs were grown to 60-70% confluence and transfected shPDE4B or NC, and cisplatin was administered after transfection. All cells were collected 24 h after treatment with cisplatin.

RNA isolation and real-time quantitative PCR. Total RNA from kidney cortex tissues and cells was isolated using TRIzol reagent (TaKaRa). cDNA was generated from 1 μg of total RNA using PrimeScript™ Reverse Transcriptase (TaKaRa Biotechnology Co., Ltd., Dalian, China). Quantitative PCR was subsequently carried out using SYBR Green Master Mix (Vazyme, Nanjing, China) on a QuantStudio 3 Real-time PCR System (Applied Biosystems, Foster City, CA, USA). The cycling program consisted of a preliminary denaturation (95°C for 10 min), followed by 40 cycles (95°C for 15 s and 60°C for 1 min).The relative mRNA levels were normalized to the levels of GAPDH and calculated using the comparative cycle threshold (ΔΔCt) method. The primer sequences are shown in Table 1.

Western blotting. Kidney cortex tissue and RTECs were lysed using RIPA buffer supplemented with protease and phosphatase inhibitors at 4°C for 30 min. The samples were centrifuged at 12,000 rpm for 5 min in a 4°C centrifuge. The protein

concentration was detected with a BCA Protein Assay Kit (Beyotime). Then, the proteins were separated by SDS-polyacrylamide gel electrophoresis and transferred onto polyvinylidene difluoride (PVDF) membranes. The PVDF membranes were then blocked in 5% nonfat dry milk with Tris-buffered saline/Tween-20 (TBST) at room temperature.

ELISA for IL-6. Serum IL-6 levels were evaluated by an ELISA kit (E-EL-M0044c, Elascience, China) according to the manufacturer's protocol.

Annexin double staining. After treatment, cells were washed three times with PBS, trypsinized and then centrifuged (1500 rpm at room temperature) for 5 min, adjusted to 5×10^4/ml and double-stained with annexin V-FITC/PI or V-PE/7-AAD (Apoptosis Detection Kit, BD Biosciences, San Diego, CA) according to the manufacturer's instructions(40). After incubation for 15 min at room temperature in the dark, the fluorescent intensity was measured using a flow cytometer (BD Biosciences, San Diego, CA). The values of Q2 and Q3 represented total apoptotic rate of cells.

Cyclic adenosine monophosphate (cAMP) measurement. The cAMP concentrations of kidney tissues were measured by an enzyme-linked immunosorbent assay (ELISA) following the manufacturer's protocol (Mouse/rat cAMP Parameter Assay Kit, KGE 012B; R&D system; Minneapolis, MN, USA)(7).

Statistical analysis. Statistical analysis was performed using GraphPad 6.0 statistical software. The results are expressed as the mean ± SEM. Statistically significant differences were determined by ANOVA followed by Bonferroni's multiple comparison test or Student's t-test using GraphPad Prism 6 software. A value of $P <$

0.05 was considered significant.

RESULTS

1. Expression of PDE4 subtypes in cisplatin-induced AKI in vivo

First, we examined the expression of PDE4 subtypes in mice with cisplatin-induced AKI by qRT-PCR and Western blotting. We found that PDE4B and PDE4D mRNA levels were both upregulated and increased 4.86-fold and 2.91-fold, respectively. However, there were no significant differences in PDE4A or PDE4C levels (Fig. 1a). The Western blotting results showed that only PDE4B protein expression was obviously increased (Fig.1b & c). Immunohistochemical result also indicated that PDE4B was increased in the kidneys of cisplatin-treated mice (Fig.1d). These results indicate that PDE4/PDE4B may play an important role in cisplatin-induced AKI.

2. Cilomilast significantly improved cisplatin-induced renal dysfunction, renal pathological damage and renal tubular injury in vivo.

It was well established that a single injection of cisplatin at a dose of 20 mg/kg body weight into mice can cause obvious renal injury, as shown by tubular cell apoptosis, necrosis, and cast formation, and lead to renal dysfunction (15) . To investigate the role of PDE4 in AKI, we pretreated mice with the PDE4 inhibitor cilomilast (30 mg/kg) and induced AKI by the intraperitoneal injection of cisplatin 20 mg/kg) 24 h later. The mice were sacrificed 72 h after cisplatin injection. Considering the important role of PDE4B in inflammation, we further examined whether PDE4B

expression is decreased after cilomilast treatment. Western blotting and quantitative analysis showed that the PDE4 inhibitor cilomilast significantly inhibited the upregulation of PDE4B protein by cisplatin (Fig. 2a & b). The reduction of PDE4A was also restored by cilomilast (Fig. 2a & c), while the dysregulation of other PDE4 subtypes was not rescued (Fig. 2a, d & e). Seventy-two hours after cisplatin injection, the reduction of cAMP in kidney tissues was significantly blunted by cilomilast treatment. (Fig. 2f). Moreover, blood urea nitrogen (BUN) and creatinine (SCr) levels were increased significantly, whereas they decreased obviously after cilomilast treatment, suggesting that cilomilast treatment improved renal function in mice with cisplatin-induced AKI (Fig. 2g & h). Consistent with the improvement of renal function, renal PAS staining indicated that cisplatin-induced renal tubular epithelial cell necrosis, basement membrane exposure, brush border disappearance, tubular dilation, and tubular cast formation were all attenuated after cilomilast treatment (Fig. 2i). Renal tubular injury scores further confirmed a significant improvement in renal pathological damage (Fig. 2j). KIM-1 and NGAL are novel markers of renal tubular injury. By qRT-PCR, we found that the levels of KIM-1 and NGAL in the cisplatin treatment group increased by 916.54-fold and 179.11-fold, respectively, while cilomilast treatment significantly inhibited the upregulation of KIM-1 and NGAL (Fig. 2k & l). Western blotting further verified the downregulatory effect of cilomilast on NGAL at the protein level (Fig. 2m & n).

3. Cilomilast significantly improved cisplatin-induced renal cell apoptosis and

inflammation in vivo

The number of TUNEL-positive cells increased significantly in cisplatin-induced AKI kidney tissue, while cilomilast reduced the number of TUNEL-positive cells (Fig. 3a). Consistent with this, the expression of the pro-apoptotic protein BAX in the renal tissue of AKI mice was also increased (mRNA and protein levels increased by 6.01-fold and 6.92-fold, respectively), and cilomilast significantly inhibited the upregulation of BAX expression (Fig. 3b, c & e). At the same time, the activation of the pro-apoptotic enzyme caspase 3 was also inhibited (Fig. 3b & d). These results reveal that the PDE4 inhibitor cilomilast improved cisplatin-induced renal cell apoptosis in AKI mice. Inflammation is also an important pathological phenomenon in the process of AKI, and it plays a vital pathological role in the occurrence and development of AKI. By qRT-PCR and ELISA, we discovered that the mRNA levels of IL-1β, IL-6, TNF-α, NLRP3, MCP-1 and serum IL-6 were elevated in cisplatin-exposed kidney tissue, while cilomilast downregulated the expression of these inflammatory factors (Fig. 3f-k), suggesting that cilomilast inhibits cisplatin-induced kidney inflammation.

4. Knocking down the PDE4B gene effectively attenuated cisplatin-induced renal dysfunction, renal pathological damage and renal tubular injury in vivo

Next, we selectively knocked down the PDE4B gene by injecting shPDE4B into the tail vein. After 36 h, the mice were given cisplatin (intraperitoneal) to induce AKI. Seventy-two hours after treatment with cisplatin, the qRT-PCR results showed that the

expression of the PDE4B gene in the kidney tissue of mice injected with shPDE4B was decreased by 39.1% compared with that in mice injected with NC(Fig. 4a), which indicated that the PDE4B gene was effectively knocked down. In addition, BUN and SCr levels declined after PDE4B were knocked down, suggesting an improvement in renal function (Fig. 4b & c). Consistent with this, renal PAS staining also showed that tubular damage was effectively ameliorated (Fig. 4d & e). By qRT-PCR, we discovered that the knockdown of the PDE4B gene significantly inhibited the upregulation of KIM-1 and NGAL (Fig. 4f & g). Western blotting further verified the downregulation of NGAL induced by the knockdown of the PDE4B gene at the protein level (Fig. 4h & i).

5. Knocking down the PDE4B gene ameliorated the pro-apoptotic effect and inflammation in mice with cisplatin-induced AKI

We found that the knockdown of PDE4B effectively reduced the number of TUNEL-positive cells induced by cisplatin (Fig. 5a), and the expression of BAX, which mediates apoptosis, was also downregulated (Fig. 5b). In addition, we performed qRT-PCR to test IL-6, IL-1β, and TNF-α mRNA levels. As shown in Fig. 5, the mRNA levels of inflammatory factors were also remarkably decreased after the PDE4B gene was knocked down (Fig. 5c-e). These results indicate that the knockdown PDE4B improves apoptosis and inflammation in mice with cisplatin-induced AKI.

6. Effect of the PDE4 inhibitor cilomilast on cisplatin-induced apoptosis and inflammation in RTECs

After the stimulation of RTECs with cisplatin for 24 h, we used qRT-PCR to detect PDE4 subtype expression. There were no significant differences in PDE4A and PDE4C at mRNA levels before or after stimulation with cisplatin, which was consistent with the changes observed in vivo. PDE4B increased 1.47-fold after cisplatin stimulation (Fig. 6a). However, PDE4D was not detected, probably due to its low expression level in RTECs. To observe whether the PDE4 inhibitor cilomilast can relieve the damage caused by cisplatin in vitro, we pretreated RTECs with cilomilast (5 μM) for 40 min and then induced cell injury with cisplatin (5 μg/ml). After 24 h, the cells were collected. Flow cytometry (annexin V-FITC/PI) was used to detect cell apoptosis. The results showed that the apoptosis rate in the cisplatin group was increased to 36.47% while the rate in the cilomilast group was significantly reduced to 22.26% (Fig. 6b & c). Consistent with the improvement in apoptosis levels, qRT-PCR confirmed that cilomilast inhibited the upregulation of cisplatin-induced BAX mRNA levels (Fig. 6d). Furthermore, we examined the expression of inflammatory factors by qRT-PCR. The results showed that cilomilast pretreatment significantly inhibited the upregulation of the inflammatory factors IL-1β (Fig. 6e) and IL-6 (Fig. 6f) compared with that in the cisplatin group. These results indicated that cilomilast can directly improve cisplatin-induced apoptosis and inflammation in RTECs.

7. Effect of PDE4B gene knockdown on cisplatin-induced apoptosis and

inflammation in RTECs

To clarify the role of PDE4B in cisplatin-induced renal tubular epithelial cell injury, we transfected RTECs with empty plasmid or shPDE4B (24 h) in vitro and then collected the cells after 24 h of stimulation with cisplatin. Flow cytometry (V-PE/7-AAD) was used to detect cell apoptosis. The results showed that knocking down PDE4B effectively ameliorated cisplatin-induced apoptosis (Fig. 7a & b). By qRT-PCR, we found that, after RTECs were transfected with shPDE4B, PDE4B expression decreased by 32.5% and cisplatin-induced PDE4B mRNA upregulation was also completely reversed (Fig. 7c). qRT-PCR results also confirmed that BAX upregulation was inhibited after PDE4B knockdown, and the downregulation of the anti-apoptotic factor Bcl-2 was partially reversed (Fig. 7d & e). These results indicate that the knockdown of PDE4B attenuates cisplatin-induced RTEC apoptosis. In addition, we used qRT-PCR to examine TNF-α, IL-6, and IL-1β levels and found that the knockdown of the PDE4B gene effectively improved cisplatin-induced RTEC inflammation (Fig. 7f-h).

8. Cilomilast increased the expression of Sirt1 and upregulated the phosphorylation of AKT after cisplatin administration in vivo

Phosphodiesterase-4 inhibitor confers neuroprotective effects through the Sirt1/AKT pathway (20) . And Sirt1 is closely involved in renal physiology and pathology (9) . We performed Western blotting to detect the expression of Sirt1. As shown in Fig. 8a-d, Sirt1 expression was remarkably downregulated in the cisplatin

group, while cilomilast administration significantly upregulated Sirt1 expression. In addition, we also observed the expression of AKT and its upstream protein molecule PI3K. The results illustrated that cilomilast rescued the phosphorylation of AKT and blunted the reduction of PI3K to some extent.

DISCUSSION

The main pathological manifestation of cisplatin-induced AKI is proximal tubular injury accompanied by oxidative stress, inflammation, apoptosis and renal vascular injury (25) . Until now, there has been no effective means for specifically preventing cisplatin-induced AKI.

As an important second messenger molecule in the cell, cAMP can further activate its downstream signaling pathway to exert its physiological functions. PDE4 can specifically hydrolyse cAMP, thereby affecting DNA repair and cell differentiation. PDE4 is also a therapeutic target for many inflammatory diseases, including asthma, COPD, inflammatory bowel disease (Crohn's disease, etc.), psoriasis, nervous system inflammation (Alzheimer's disease, depression, multiple sclerosis, etc.) and rheumatoid arthritis(19) .

PDE4 inhibitors have been shown to have potential therapeutic effects in a number of diseases. In neurological diseases, PDE4 inhibitors can attenuate neuronal apoptosis in early brain injury (20) . Kosutova found that, in acute lung injury, the inhibition of PDE4 inhibits apoptosis of lung epithelial cells, decreases caspase-3 activation, and decreases the number of caspase-3-positive cells in lung tissue(17) . In

our study, a PDE4 inhibitor significantly improved cisplatin-induced renal dysfunction, renal pathological damage, acute tubular injury, apoptosis, and the inflammatory response, suggesting that the upregulation and activation of PDE4 may be involved in the occurrence and development of AKI.

PDE4 has four subtypes. Researchers found that PDE4A and PDE4B expression increases while PDE4C and PDE4D expression shows no obvious change in a renal fibrosis model(6). According to our results, PDE4B expression was upregulated in the kidneys of cisplatin-induced AKI mice, while the protein levels of other PDE4 subtypes were downregulated. The expression of PDE4 subtypes is not completely consistent under different disease states and models(12) . They may also be related to the different functions performed by each subtype in different diseases(34). Researchers found that the expression of PDE4D mRNA does not always correlate with the pattern of protein expression(32). Some researchers also found that another member of PDE family, PDE5, has three conformational forms, and band 2 PDE5 could be converted to band 3 PDE5 by PDE5-specific inhibitors(4). However, whether a similar conversion also exists in PDE4 subtypes needs further investigation.

Researchers have found that, in mouse peritoneal macrophages, the expression of PDE4A, PDE4B, and PDE4D is upregulated after stimulation with LPS but that the increase in PDE4B is most significant(13) ; The expression of the other two subtypes is not affected by the knockdown one subtype, which indicates that the three subtypes may be functionally independent and do not overlap each other. Further studies have found that LPS-induced TNF-α expression is only reduced in PDE4B knockout mice

among PDE4 subtype knockout mice, suggesting a unique role for PDE4B in inflammation(13) . Considering the important role of PDE4B in the inflammatory process and its consistent upregulation in AKI and CKD, we specifically silenced the PDE4B gene in vivo and observed its role in cisplatin-induced AKI.

Consistent with the results of intervention with the inhibitor, we found that after, knocking down PDE4B, cisplatin-induced renal damage was improved significantly, and the upregulation of the inflammatory factors TNF-α, IL-6, and IL-1β was almost completely reversed. This suggests that this intervention may protect the kidneys by antagonizing the effects of inflammation. Consistent with our findings, PDE4B knockout ($PDE4B^{-/-}$ mice) and PDE4 inhibitor roliplam, significantly alleviate alcohol-related neuroinflammation(1) , and PDE4B is considered an effective target for treating nervous system inflammation(29) . Researchers have designed a drug that specifically inhibits PDE4B and found that it can improve the inflammatory response in inflammatory diseases of the skin(30) , but the role of the drug in other inflammatory diseases and its potential for clinical application requires further research and observation.

The renal protection confirmed in vivo is the result of systemic intervention and lacks cell or tissue specificity. It may be the result of interventions on renal cell PDE4/PDE4B, or it may be due to the secondary effects of the inhibition of other cells that express PDE4/PDE4B, such as immune cells and vascular cells. AKI is often considered to be the result of multiple factors and is characterized by the death of renal tubular epithelial cells (RTECs). The protection of renal tubular epithelial cells

plays an important role in the prevention and treatment of AKI.

Our in vitro results demonstrate that PDE4 inhibitors have a significant protective effect against cisplatin-induced RTEC injury. We found that, after the PDE4B gene was knocked down, cisplatin-induced apoptosis and inflammation in tubular epithelial cells were also improved. Therefore, we speculated that the specific inhibition of PDE4/PDE4B in renal tubular epithelial cells may be an effective strategy for prevention and treatment of AKI.A large number of studies have also shown that immune cell activation and vascular cell damage, in addition to renal tubular epithelial cells, are involved in the occurrence and development of AKI. T lymphocytes, especially CD4+ T cells, are one of the important cell types involved in renal ischemia-reperfusion injury (IRI), and CD4+ T cell-deficient mice show milder kidney damage after IRI(3, 31) . Perivascular capillary (PTC) endothelial damage can also aggravate the extent of kidney damage and lead to local renal hypoxia after IRI(18, 28) . In future studies, it is necessary to specifically knock-down PDE4B in renal tubular cells, immune cells or vascular endothelial cells, and observe the role of PDE4B in renal damage induced by cisplatin in different cells.

The mechanism by which PDE4 inhibitors attenuate cisplatin-induced AKI is not well understood. Some reports have suggested that inhibiting PDE4 activity and inducing cAMP signaling can increase Sirt1 activity to protect cells(27) . An impressive number of scientific experiments have indicated that Sirt1 plays an important role in preventing acute kidney injury(9). Overexpressing Sirt1 in proximal tubules can rescue cisplatin-induced AKI by maintaining peroxisome number and

function, concomitantly upregulating catalase, and eliminating renal ROS(10) . Sirt1 regulates gene expression through the deacetylation of histones and non-histones at the transcriptional and post-transcriptional levels. Phosphatidylinositol-3-kinase (PI3K) is a lipid kinase, that generates phosphatidylinositol-3,4,5-trisphosphate (PI(3, 4, 5)P3).PI(3, 4, 5)P3 is a second messenger essential for the translocation of AKT to the plasma membrane, where it is phosphorylated and activated by phosphoinositide-dependent kinase 1 (PDK 1) and PDK2. The activation of AKT plays a vital role in fundamental cellular functions such as cell survival and proliferation by phosphorylating a variety of substrates(24) . Researchers have also found that Sirt1 deacetylation enhances the binding of AKT and PDK1 to PIP3 and promotes their activation(38) . Our results showed that Sirt1, PI3K and pAKT protein expression increases after cilomilast treatment and that the renal function is well protected. PDE4 inhibitors activate Sirt1 expression, increase AKT phosphorylation, and attenuate apoptosis in injured neurons(20). In LPS-induced AKI, the activation of Sirt1 inhibits the NF-κB signaling pathway, thereby attenuating renal inflammation(41) . Studies have also verified that the PI3K-Akt signaling pathway, is required for the induction of Sirt1 expression by endoplasmic reticulum stress(16) .In our experiments, the activation of Sirt1 by a PDE4 inhibitor may have directly activated the PI3K/AKT signaling pathway, or it may have been a secondary outcome of treatment with the PDE4 inhibitor; the mechanism needs to be further clarified in future studies.

GRANTS

This work was supported by grants from the National Natural Science Foundation of China (81625004, 81830020, 81530023, 81700604, 81570616, 81670647, 81873599, and 81800598), the National Key Research and Development Program (2016YFC0906103), the Natural Science Foundation of Jiangsu Province (SBK2017041428), and the Postgraduate Research & Practice Innovation Program of Jiangsu Province (KYCX18_1499).

AUTHOR CONTRIBUTIONS

Z. J., X.Y., and M.X. designed the study. X.M., X.Y., and X. M. performed experiments. X.Y., X.M., and Z.J. analyzed the data. Z.J., S.H., Y.Z., and A.Z. interpreted the results. M.X., X.Y., and Z.J. wrote the manuscript.

DISCLOSURE

The authors declare no conflicts of interests.

References:

1. **Avila DV, Myers SA, Zhang J, Kharebava G, McClain CJ, Kim HY, Whittemore SR, Gobejishvili L, and Barve S**. Phosphodiesterase 4b expression plays a major role in alcohol-induced neuro-inflammation. *Neuropharmacology* 125: 376-385, 2017.
2. **Basile DP, Bonventre JV, Mehta R, Nangaku M, Unwin R, Rosner MH, Kellum JA, and Ronco C**. Progression after AKI: Understanding Maladaptive Repair Processes to Predict and Identify Therapeutic Treatments. *J Am Soc Nephrol* 27: 687-697, 2016.
3. **Burne MJ, Daniels F, El GA, Mauiyyedi S, Colvin RB, O'Donnell MP, and Rabb H**. Identification of the CD4(+) T cell as a major pathogenic factor in ischemic acute renal failure. *J Clin Invest* 108: 1283-1290, 2001.
4. **Corbin JD, and Francis SH**. Conformational conversion of PDE5 by incubation with sildenafil or

metal ion is accompanied by stimulation of allosteric cGMP binding. *Cell Signal* 23: 1578-1583, 2011.
5. **Diamant Z, and Spina D**. PDE4-inhibitors: a novel, targeted therapy for obstructive airways disease. *Pulm Pharmacol Ther* 24: 353-360, 2011.
6. **Ding H, Bai F, Cao H, Xu J, Fang L, Wu J, Yuan Q, Zhou Y, Sun Q, He W, Dai C, Zen K, Jiang L, and Yang J**. PDE/cAMP/Epac/C/EBP-beta Signaling Cascade Regulates Mitochondria Biogenesis of Tubular Epithelial Cells in Renal Fibrosis. *Antioxid Redox Signal* 29: 637-652, 2018.
7. **Eiam-Ong S, Nakchui Y, Chaipipat M, and Eiam-Ong S**. Vanadate-Induced Renal cAMP and Malondialdehyde Accumulation Suppresses Alpha 1 Sodium Potassium Adenosine Triphosphatase Protein Levels. *Toxicol Res* 34: 143-150, 2018.
8. **Fan CK**. Phosphodiesterase inhibitors in airways disease. *Eur J Pharmacol* 533: 110-117, 2006.
9. **Guan Y, and Hao CM**. SIRT1 and Kidney Function. *Kidney Dis (Basel)* 1: 258-265, 2016.
10. **Hasegawa K, Wakino S, Yoshioka K, Tatematsu S, Hara Y, Minakuchi H, Sueyasu K, Washida N, Tokuyama H, Tzukerman M, Skorecki K, Hayashi K, and Itoh H**. Kidney-specific overexpression of Sirt1 protects against acute kidney injury by retaining peroxisome function. *J Biol Chem* 285: 13045-13056, 2010.
11. **Houslay MD**. PDE4 cAMP-specific phosphodiesterases. *Prog Nucleic Acid Res Mol Biol* 69: 249-315, 2001.
12. **Jacob C, Leport M, Szilagyi C, Allen JM, Bertrand C, and Lagente V**. DMSO-treated HL60 cells: a model of neutrophil-like cells mainly expressing PDE4B subtype. *Int Immunopharmacol* 2: 1647-1656, 2002.
13. **Jin SL, Lan L, Zoudilova M, and Conti M**. Specific role of phosphodiesterase 4B in lipopolysaccharide-induced signaling in mouse macrophages. *J Immunol* 175: 1523-1531, 2005.
14. **Jin SL, and Conti M**. Induction of the cyclic nucleotide phosphodiesterase PDE4B is essential for LPS-activated TNF-alpha responses. *Proc Natl Acad Sci U S A* 99: 7628-7633, 2002.
15. **Kim YJ, Lee MY, Son HY, Park BK, Ryu SY, and Jung JY**. Red ginseng ameliorates acute cisplatin-induced nephropathy. *Planta Med* 80: 645-654, 2014.
16. **Koga T, Suico MA, Shimasaki S, Watanabe E, Kai Y, Koyama K, Omachi K, Morino-Koga S, Sato T, Shuto T, Mori K, Hino S, Nakao M, and Kai H**. Endoplasmic Reticulum (ER) Stress Induces Sirtuin 1 (SIRT1) Expression via the PI3K-Akt-GSK3beta Signaling Pathway and Promotes Hepatocellular Injury. *J Biol Chem* 290: 30366-30374, 2015.
17. **Kosutova P, Mikolka P, Kolomaznik M, Balentova S, Adamkov M, Calkovska A, and Mokra D**. Reduction of lung inflammation, oxidative stress and apoptosis by the PDE4 inhibitor roflumilast in experimental model of acute lung injury. *Physiol Res* 67: S645-S654, 2018.
18. **Le Dorze M, Legrand M, Payen D, and Ince C**. The role of the microcirculation in acute kidney injury. *Curr Opin Crit Care* 15: 503-508, 2009.
19. **Li H, Zuo J, and Tang W**. Phosphodiesterase-4 Inhibitors for the Treatment of Inflammatory Diseases. *Front Pharmacol* 9: 1048, 2018.
20. **Li Q, Peng Y, Fan L, Xu H, He P, Cao S, Li J, Chen T, Ruan W, and Chen G**. Phosphodiesterase-4 inhibition confers a neuroprotective efficacy against early brain injury following experimental subarachnoid hemorrhage in rats by attenuating neuronal apoptosis through the SIRT1/Akt pathway. *Biomed Pharmacother* 99: 947-955, 2018.
21. **Lipworth BJ**. Phosphodiesterase-4 inhibitors for asthma and chronic obstructive pulmonary disease. *Lancet* 365: 167-175, 2005.
22. **Myers SA, Gobejishvili L, Saraswat OS, Garrett WC, Andres KR, Riegler AS, Donde H,**

Joshi-Barve S, Barve S, and Whittemore SR. Following spinal cord injury, PDE4B drives an acute, local inflammatory response and a chronic, systemic response exacerbated by gut dysbiosis and endotoxemia. *Neurobiol Dis* 124: 353-363, 2019.

23. **Okusa MD, Linden J, Huang L, Rosin DL, Smith DF, and Sullivan G**. Enhanced protection from renal ischemia-reperfusion [correction of ischemia:reperfusion] injury with A(2A)-adenosine receptor activation and PDE 4 inhibition. *Kidney Int* 59: 2114-2125, 2001.

24. **Osaki M, Oshimura M, and Ito H**. PI3K-Akt pathway: its functions and alterations in human cancer. *Apoptosis* 9: 667-676, 2004.

25. **Ozkok A, and Edelstein CL**. Pathophysiology of cisplatin-induced acute kidney injury. *Biomed Res Int* 2014: 967826, 2014.

26. **Pabla N, and Dong Z**. Cisplatin nephrotoxicity: mechanisms and renoprotective strategies. *Kidney Int* 73: 994-1007, 2008.

27. **Park SJ, Ahmad F, Philp A, Baar K, Williams T, Luo H, Ke H, Rehmann H, Taussig R, Brown AL, Kim MK, Beaven MA, Burgin AB, Manganiello V, and Chung JH**. Resveratrol ameliorates aging-related metabolic phenotypes by inhibiting cAMP phosphodiesterases. *Cell* 148: 421-433, 2012.

28. **Patschan D, Patschan S, and Muller GA**. Inflammation and microvasculopathy in renal ischemia reperfusion injury. *J Transplant* 2012: 764154, 2012.

29. **Pearse DD, and Hughes ZA**. PDE4B as a microglia target to reduce neuroinflammation. *Glia* 64: 1698-1709, 2016.

30. **Purushothaman B, Arumugam P, and Song JM**. A Novel Catecholopyrimidine Based Small Molecule PDE4B Inhibitor Suppresses Inflammatory Cytokines in Atopic Mice. *Front Pharmacol* 9: 485, 2018.

31. **Rabb H, Daniels F, O'Donnell M, Haq M, Saba SR, Keane W, and Tang WW**. Pathophysiological role of T lymphocytes in renal ischemia-reperfusion injury in mice. *Am J Physiol Renal Physiol* 279: F525-F531, 2000.

32. **Richter W, Jin SL, and Conti M**. Splice variants of the cyclic nucleotide phosphodiesterase PDE4D are differentially expressed and regulated in rat tissue. *Biochem J* 388: 803-811, 2005.

33. **Sassone-Corsi P**. The cyclic AMP pathway. *Cold Spring Harb Perspect Biol* 4: 2012.

34. **Schafer PH, Truzzi F, Parton A, Wu L, Kosek J, Zhang LH, Horan G, Saltari A, Quadri M, Lotti R, Marconi A, and Pincelli C**. Phosphodiesterase 4 in inflammatory diseases: Effects of apremilast in psoriatic blood and in dermal myofibroblasts through the PDE4/CD271 complex. *Cell Signal* 28: 753-763, 2016.

35. **Soderling SH, and Beavo JA**. Regulation of cAMP and cGMP signaling: new phosphodiesterases and new functions. *Curr Opin Cell Biol* 12: 174-179, 2000.

36. **Souness JE, Aldous D, and Sargent C**. Immunosuppressive and anti-inflammatory effects of cyclic AMP phosphodiesterase (PDE) type 4 inhibitors. *Immunopharmacology* 47: 127-162, 2000.

37. **Spina D**. PDE4 inhibitors: current status. *Br J Pharmacol* 155: 308-315, 2008.

38. **Sundaresan NR, Pillai VB, Wolfgeher D, Samant S, Vasudevan P, Parekh V, Raghuraman H, Cunningham JM, Gupta M, and Gupta MP**. The deacetylase SIRT1 promotes membrane localization and activation of Akt and PDK1 during tumorigenesis and cardiac hypertrophy. *Sci Signal* 4: a46, 2011.

39. **Wang P, Wu P, Ohleth KM, Egan RW, and Billah MM**. Phosphodiesterase 4B2 is the predominant phosphodiesterase species and undergoes differential regulation of gene expression in human monocytes and neutrophils. *Mol Pharmacol* 56: 170-174, 1999.

40. **Yang Y, Yu X, Zhang Y, Ding G, Zhu C, Huang S, Jia Z, and Zhang A**. Hypoxia-inducible

factor prolyl hydroxylase inhibitor roxadustat (FG-4592) protects against cisplatin-induced acute kidney injury. *Clin Sci (Lond)* 132: 825-838, 2018.

41. **Zhang J, Yang S, Chen F, Li H, and Chen B**. Ginkgetin aglycone ameliorates LPS-induced acute kidney injury by activating SIRT1 via inhibiting the NF-kappaB signaling pathway. *Cell Biosci* 7: 44, 2017.

FIGURE LEGENDS

Fig. 1. Expression changes of different PDE4 subtypes in the kidneys of mice with cisplatin-induced AKI (sham=6, cisplatin=8). (a) qRT-PCR analysis of the expression of the PDE4 subtypes; (b) Western blotting analysis of the expression of PDE4 subtypes. (c) Densitometry of the Western blotting in b. (d) Immunohistochemical detection of PDE4B expression (magnification: 200 ×).

Fig. 2. Effect of the PDE4 inhibitor cilomilast on cisplatin-induced renal function, renal pathology and renal tubular injury in vivo (sham=6, cisplatin=8, cilo + cisplatin=8). (a) Western blotting analysis of PDE4 expression. (b-e) Densitometry of the Western blotting in a. (f) cAMP of kidney tissue was detected by ELISA. (g) Blood urea nitrogen levels. (h) Serum creatinine levels. (i) Renal tissue PAS staining. (j) Renal tubular injury score. (k) qRT-PCR analysis of KIM-1 expression. (l) qRT-PCR analysis of NGAL expression. (m) Western blotting analysis of NGAL expression. (n) Densitometry of the Western blotting in m. *, $p < 0.05$, **, $p<0.01$ ***, $p<0.001$.

Fig. 3. Effect of the PDE4 inhibitor cilomilast on cisplatin-induced apoptosis and

inflammation in vivo (sham=6, cisplatin=8, cilo + cisplatin=8). (a) Laser confocal observation of TUNEL staining in renal tissue (magnification 630×). (b) Western blotting analysis of BAX, caspase-3, and cleaved-caspase-3 expression. (c & d) Densitometry of the Western blotting in b. (e) qRT-PCR analysis of BAX expression. (f-j) qRT-PCR was used to detect the expression of IL-6, IL-1β, TNF-α, MCP-1 and NLRP3 in kidney tissue. (k) ELISA was used to detect serum IL-6. *, $p<0.05$; **, $p < 0.01$; ***, $p < 0.001$.

Fig. 4. Effect of knocking down PDE4B on cisplatin-induced renal function, renal pathology and renal tubular injury in vivo (n=6 in each group). (a) qRT-PCR analysis of PDE4B expression in kidney tissue after the injection of shPDE4B into mice. (b) Blood urea nitrogen levels. (c) Blood creatinine levels. (d) Renal tissue PAS staining. (e) Renal tubular injury score. (f) qRT-PCR analysis of KIM-1 expression. (g) qRT-PCR analysis of NGAL expression. (h) Western blotting analysis of NGAL expression. (i) Densitometry of the Western blotting in h; *, $p<0.05$; **, $p < 0.01$; ***, $p<0.001$.

Fig. 5. Effect of PDE4B knockdown on cisplatin-induced apoptosis and inflammation in vivo (n=6 in each group). (a) Laser confocal observation of TUNEL staining in renal tissue (magnification: 630 ×). (b) qRT-PCR analysis of BAX expression. (c-e) qRT-PCR analysis of IL-6, IL-1β, and TNF-α expression. $p < 0.05$; **, $p < 0.01$; ***, $p < 0.001$.

Fig. 6. Effect of the PDE4 inhibitor cilomilast on cisplatin-induced apoptosis and inflammation in RTECs (n=3 in each group)**.** (a) qRT-PCR analysis of the expression of each subtype of PDE4; PDE4D was not detected. (b & c) Flow cytometry was used to detect apoptosis. (d) qRT-PCR was used to detect BAX expression. (e-g) qRT-PCR was used to detect IL-1β, IL-6 and TNF-α expression. $p < 0.05$; **, $p < 0.01$, ***, $p < 0.001$.

Fig. 7. Effect of PDE4B knockdown on cisplatin-induced RTEC apoptosis and inflammation (n=3 in each group)**.** (a & b) Flow cytometry was used to detect apoptosis. (c) qRT-PCR analysis of PDE4B expression. (d & e) qRT-PCR analysis of BAX and Bcl-2 expression. (f-h) qRT-PCR analysis of TNF-α, IL-6, IL-1β expression. *, $p< 0.05$; **, $p < 0.01$, ***, $p < 0.001$.

Fig. 8. Effects of cilomilast on the phosphorylation of AKT and the expression of Sirt1 (n=3 in each group). (a)Western blotting analysis of Sirt1, PI3K, p-AKT, AKT expression. (b-d) Densitometry of the Western blotting in a. *, $p< 0.05$; **, $p < 0.01$, ***, $p < 0.001$.

629

630 Table 1. Sequences of the primers for qRT-PCR.

Gene	Primer Sequence (5′-3′)
PDE4A	F: CGATGAAGCCCACCTGAGACT
	R: CCCTGGAGCTGTACCGACAAT
PDE4B	F: GTCCCTCAGAATCCTCTTCCTCAA
	R: TATGATACCCCAGAGCCCTTCC
PDE4C	F: GCTGCCTGTTGACTGCTGTGC
	R: ACATGATTGTCACGCCCTTCG
PDE4D	F: CTCCTCTGTGATGGTGGCTTT
	R: ACTTGATTGTGACCCCGTTTG
IL-1β	F: TGTGTTTTCCTCCTTGCCTCTGAT
	R: TGCTGCCTAATGTCCCCTTGAAT
IL-6	F: TCACAGAAGGAGTGGCTAAGGACC
	R: ACGCACTAGGTTTGCCGAGTAGAT
TNF-α	F: CAGACCCTCACACTCACAAACCAC
	R: CCTTGTCCCTTGAAGAGAACCTG
MCP-1	F: GTGCTGACCCCAAGAAGGAATG
	R: TGAGGTGGTTGTGGAAAAGGTAGTG
NLRP-3	F: GTCTGGAAGAACAGGCAACAT
	R: AGAACTGTCATAGGGTCAAAACG
BAX	F: AAAGTAGAAGAGGGCAACCAC
	R: CCAGGATGCGTCCACCAA
Bcl-2	F: AGGCTGGAAGGAGAAGAT
	R: CGGGAGAACAGGGTATGA
KIM-1	F: GTTGTACCGACTGCTCTT
	R: CGCTGTGGATTCTTATGT
NGAL	F: ACACTCACCACCCATTCA
	R: CACCACGGACTACAACCA

GAPDH	F:	AAGAAGGTGGTGAAGCAGG
	R:	GAAGGTGGAAGAGTGGGAGT

631

632

Figure 1

a

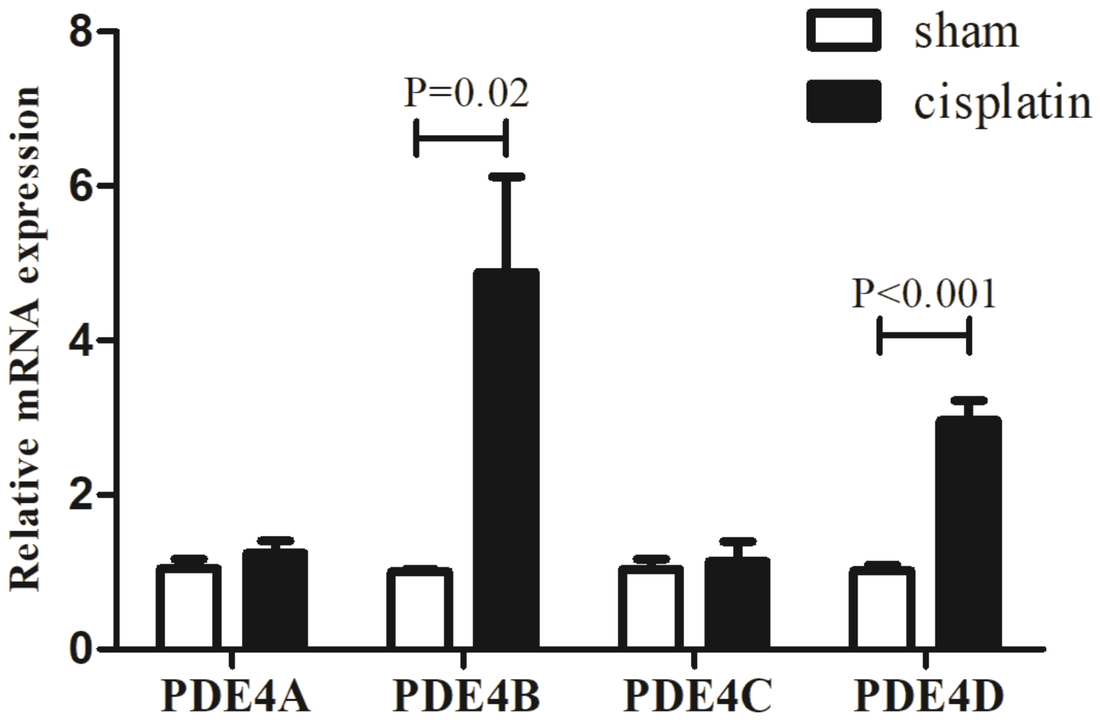

b

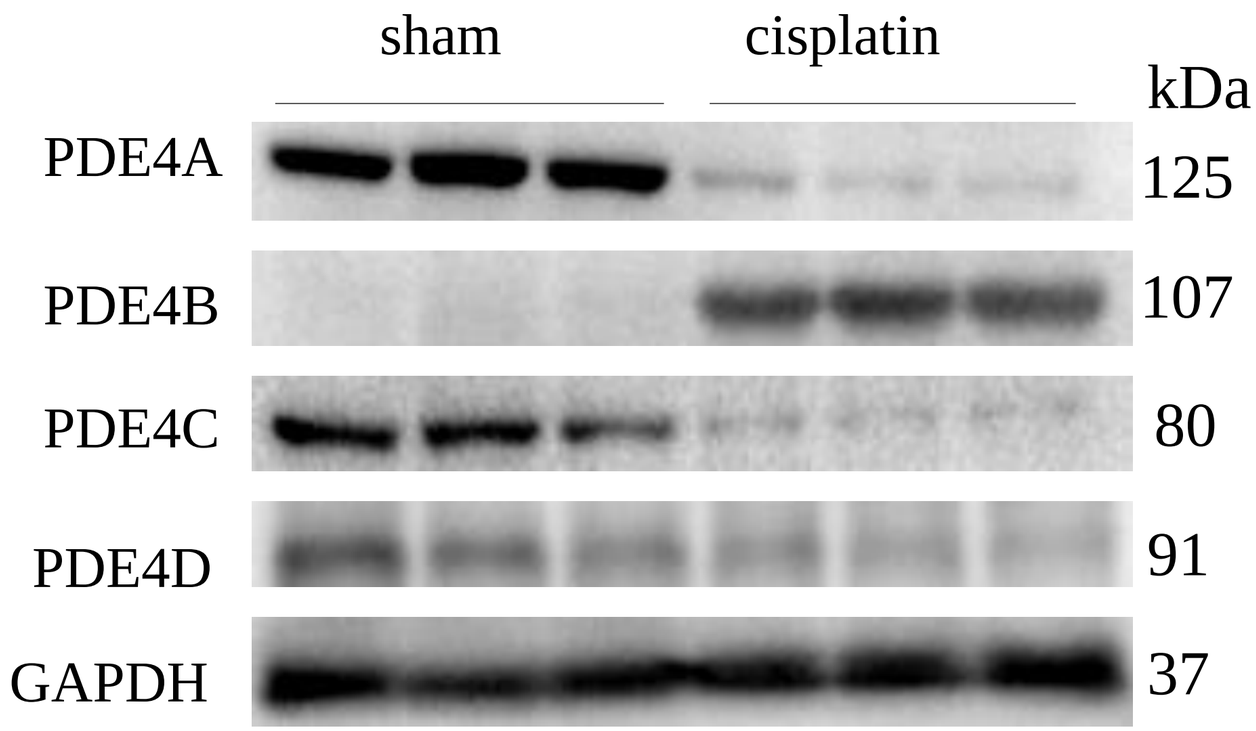

c

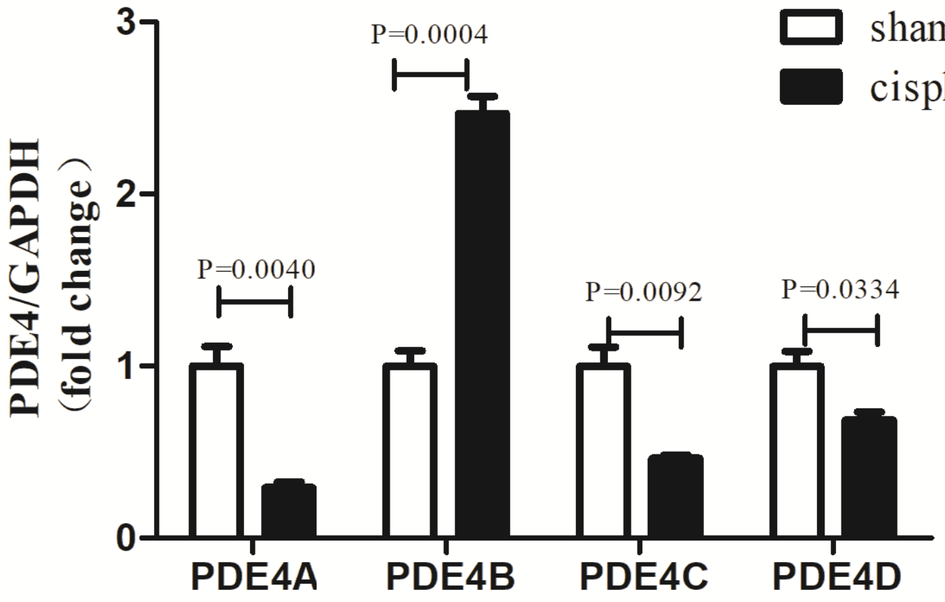

d

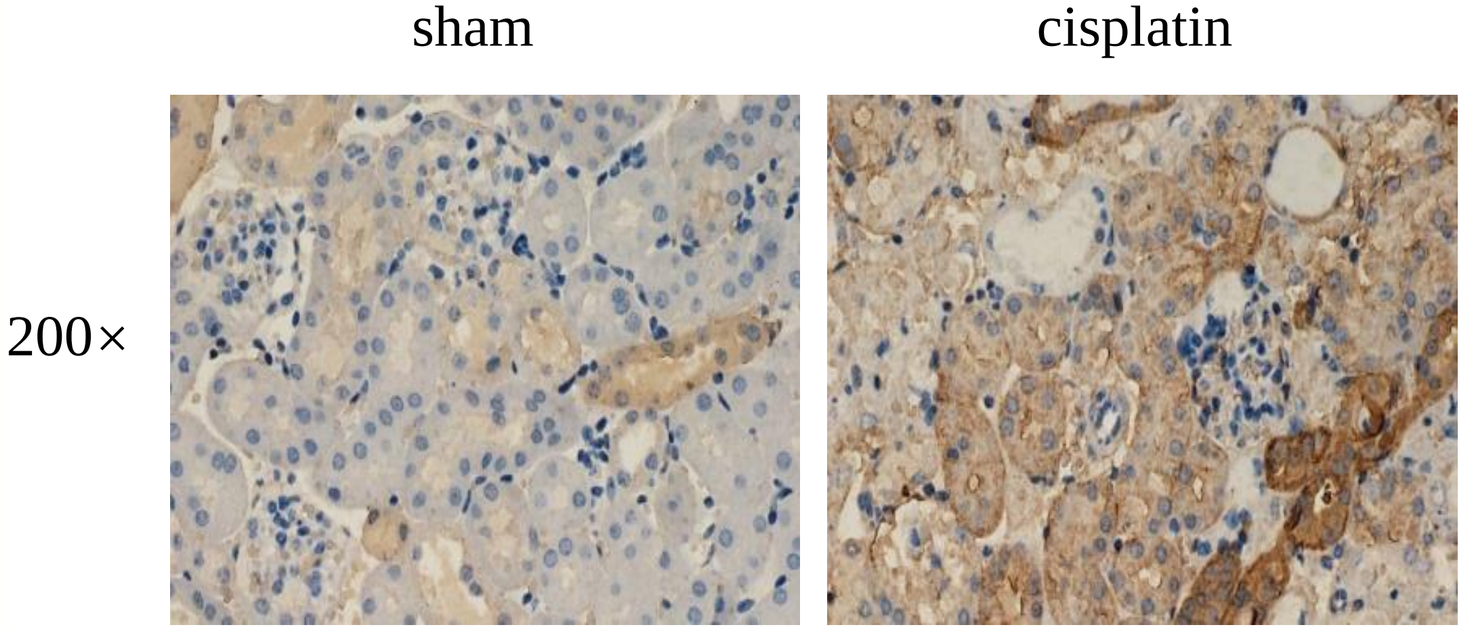

Figure 2

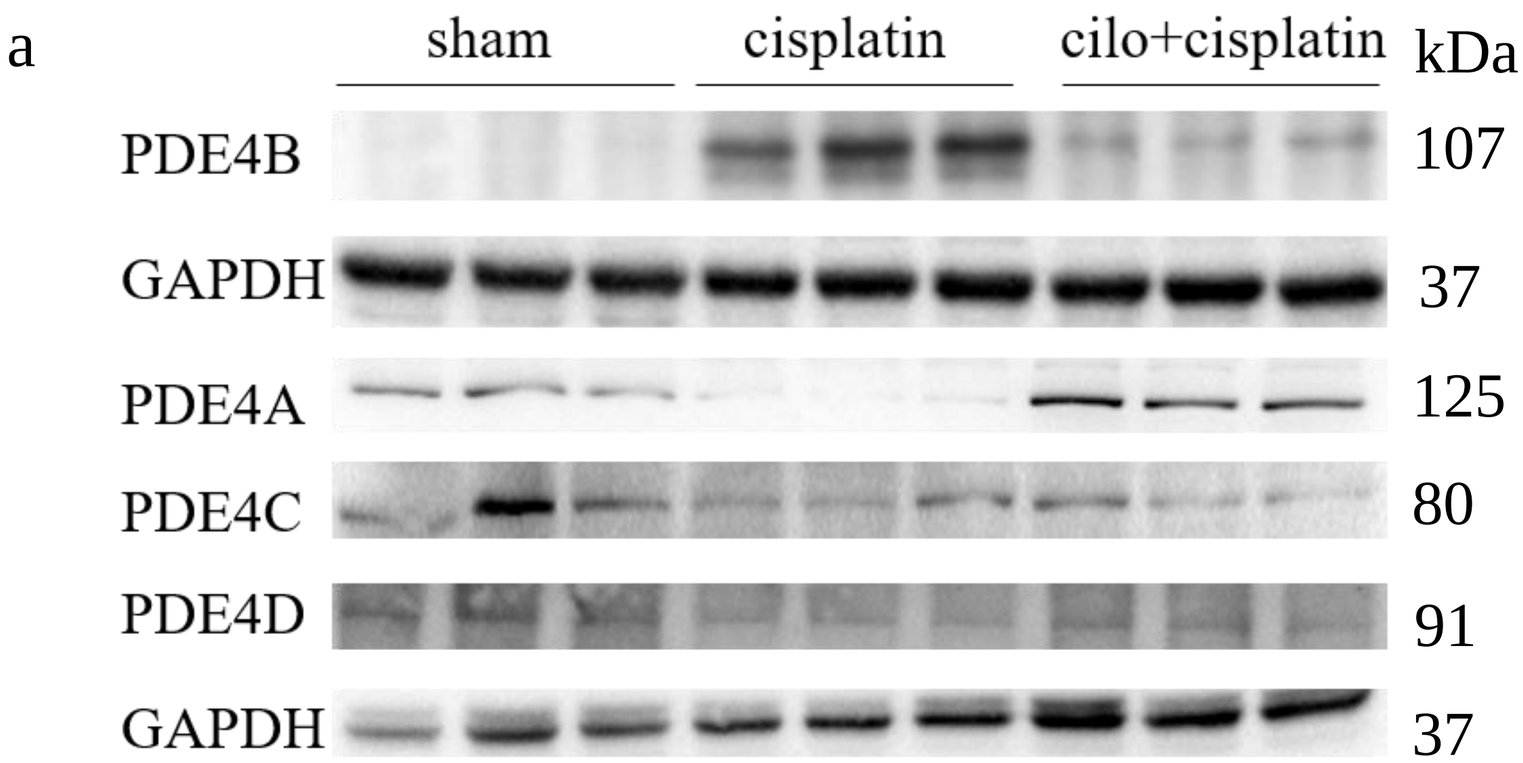

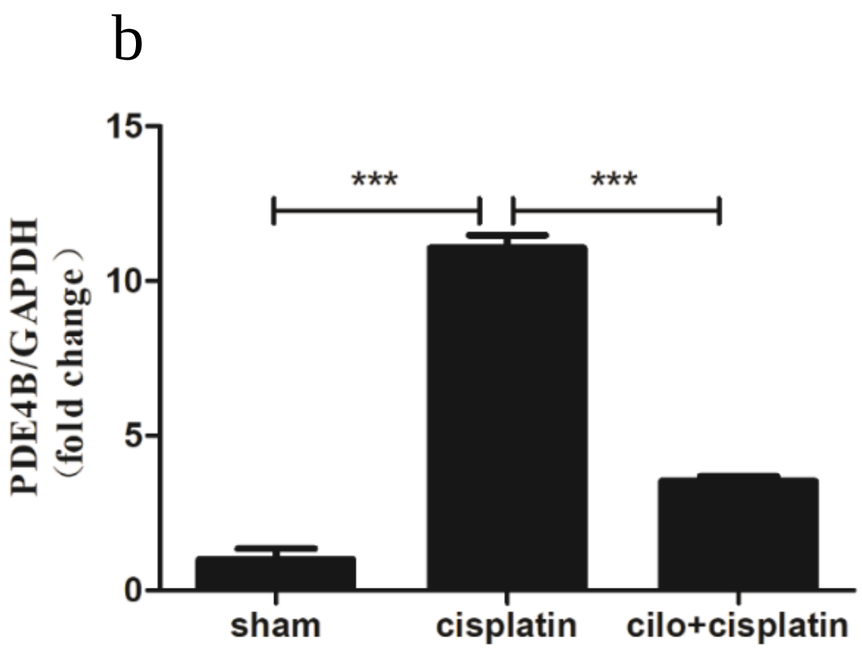

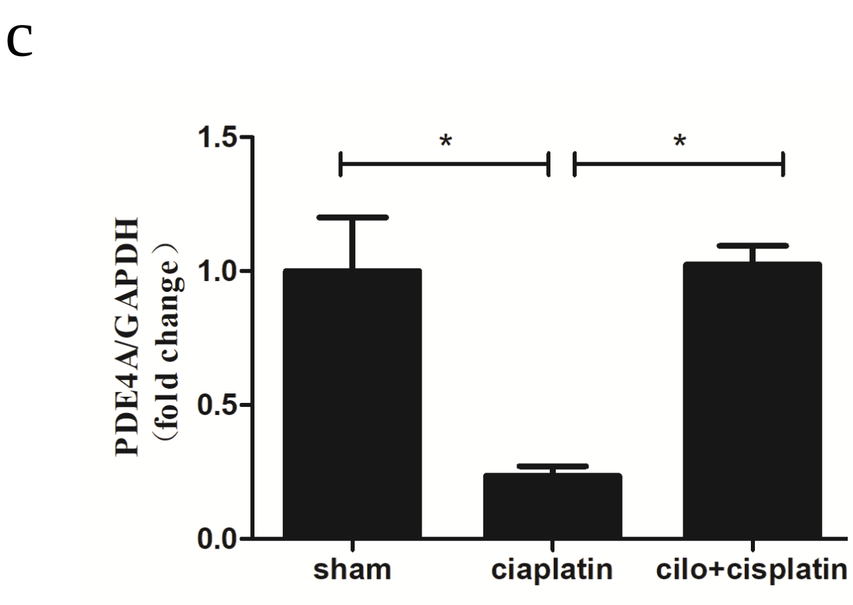

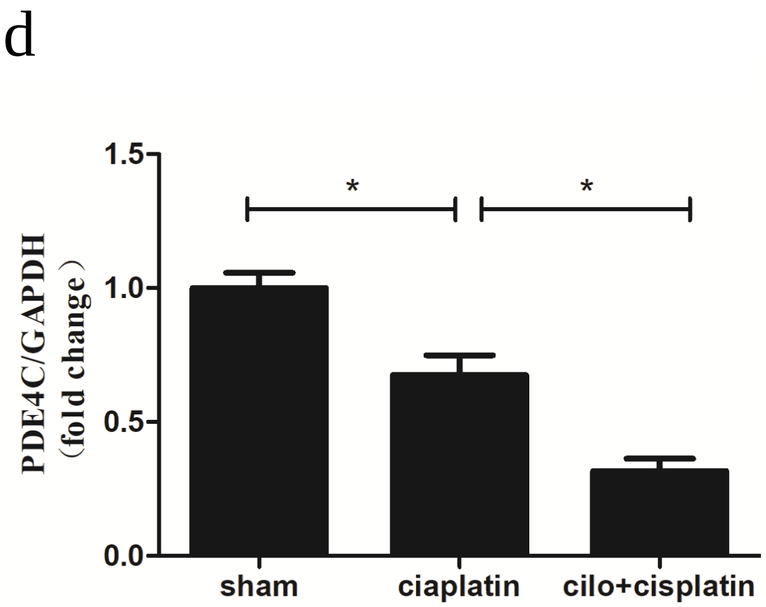

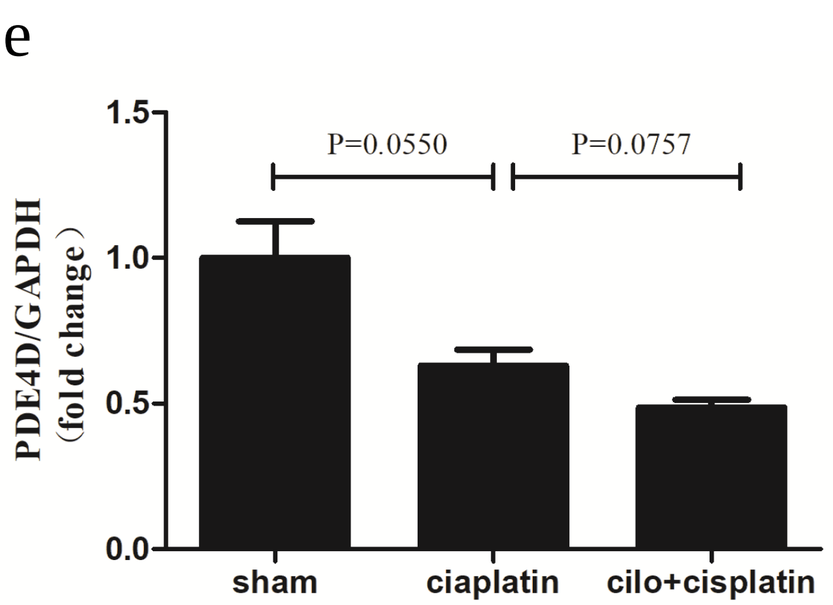

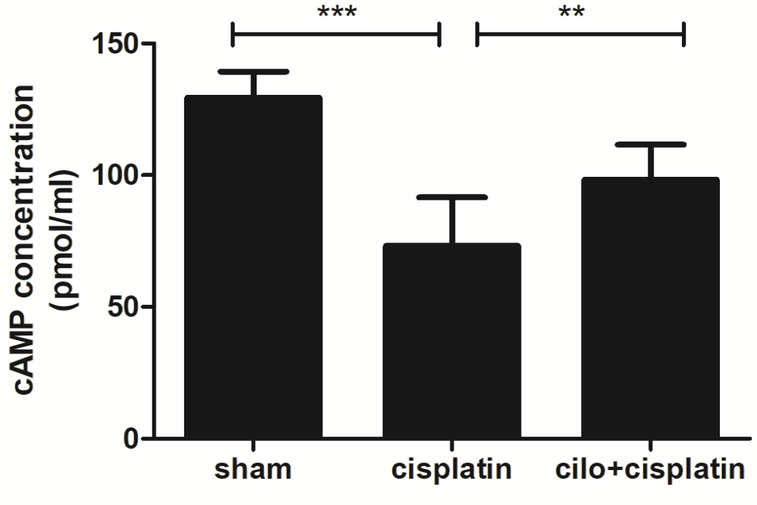

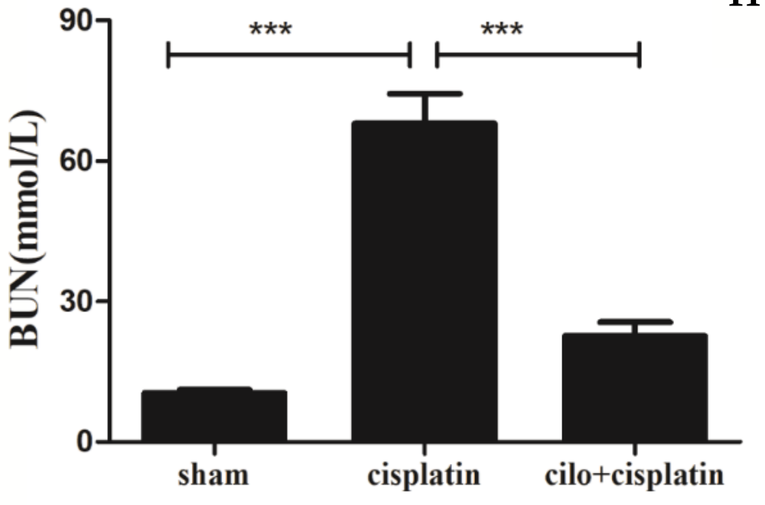

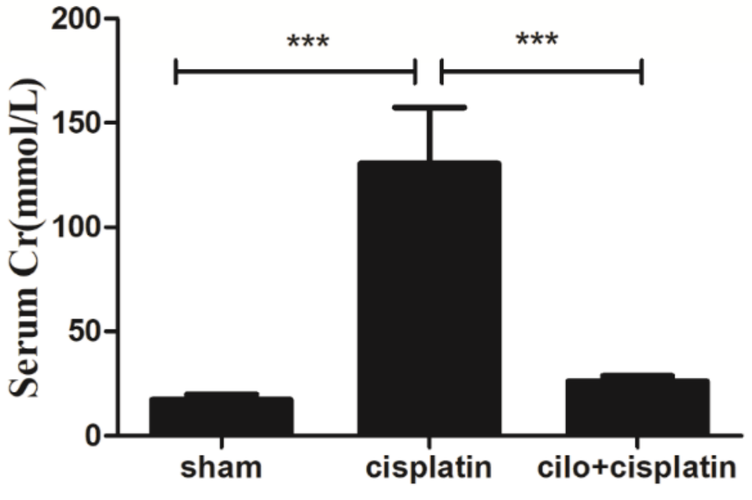

i

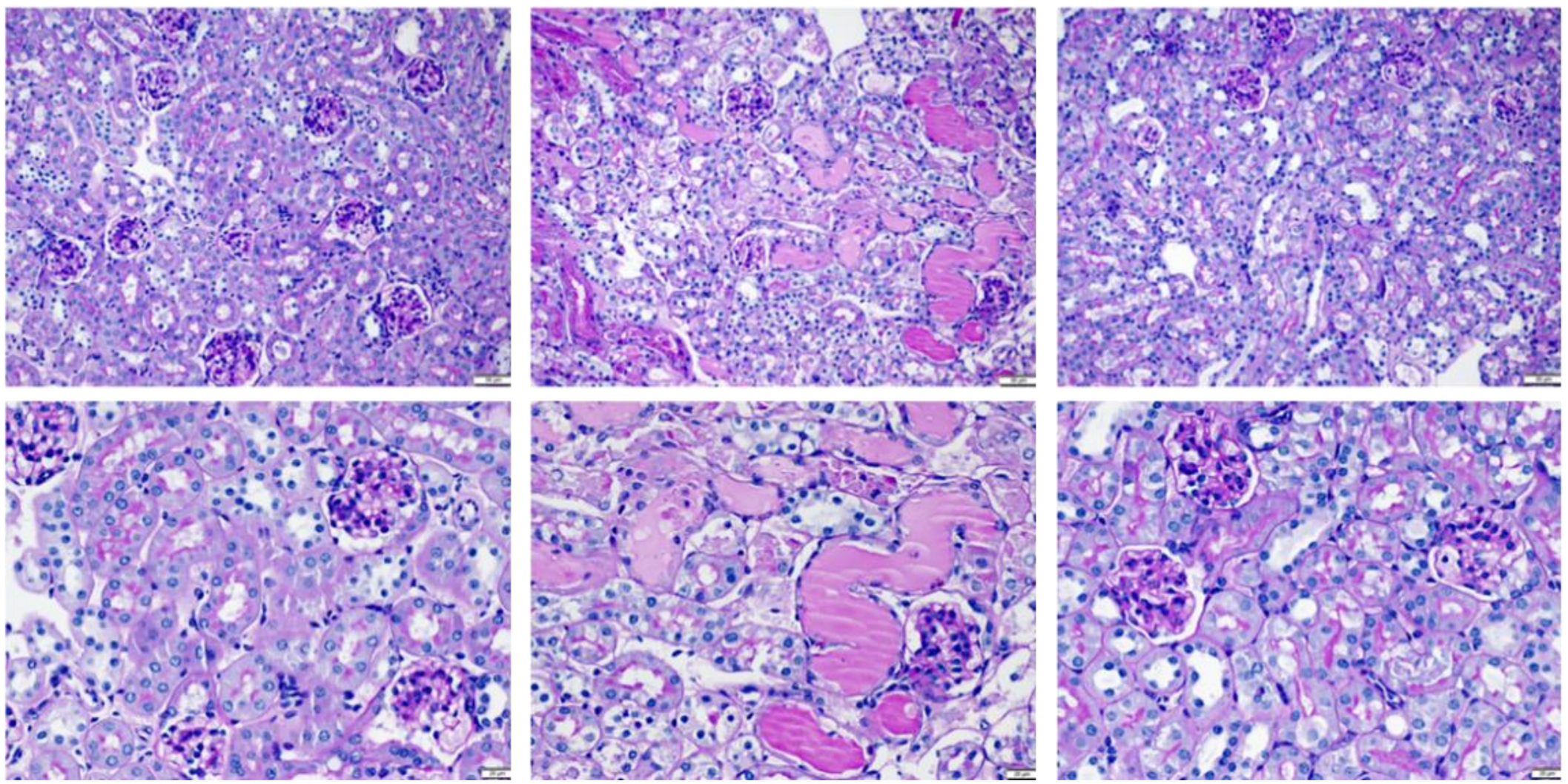

j

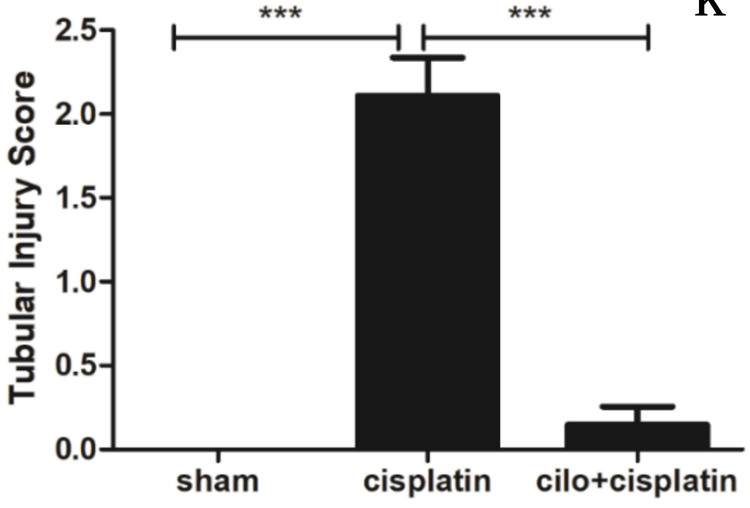

k

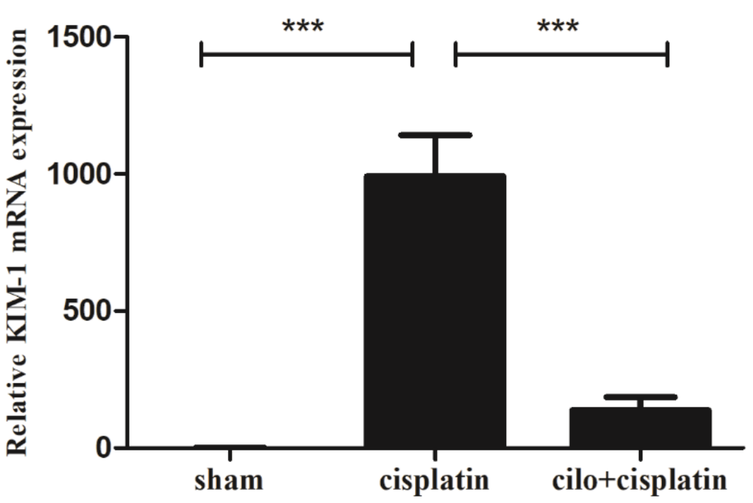

l

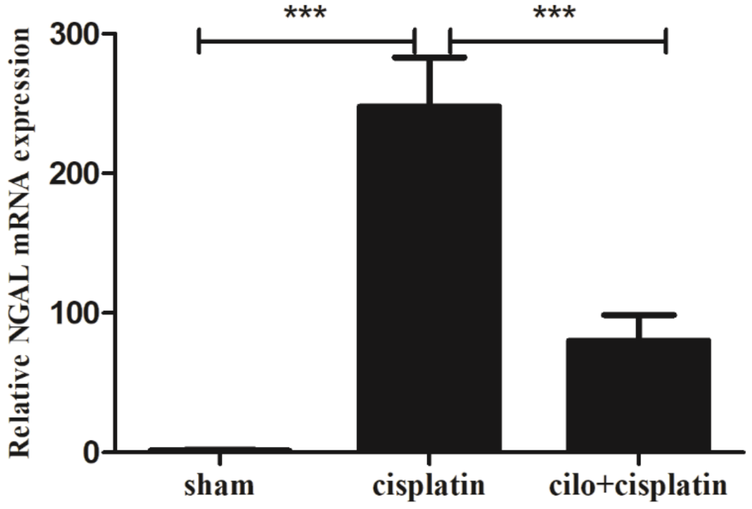

m

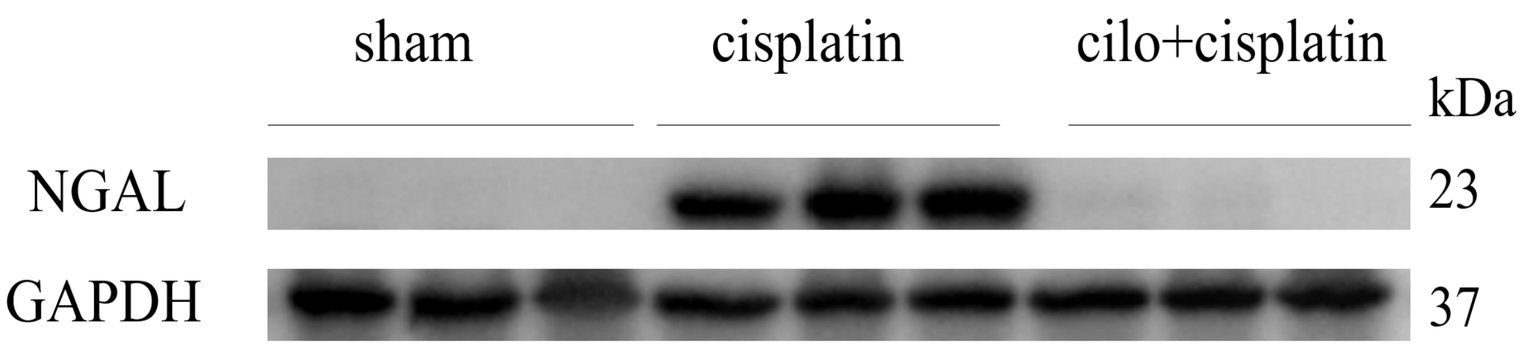

n

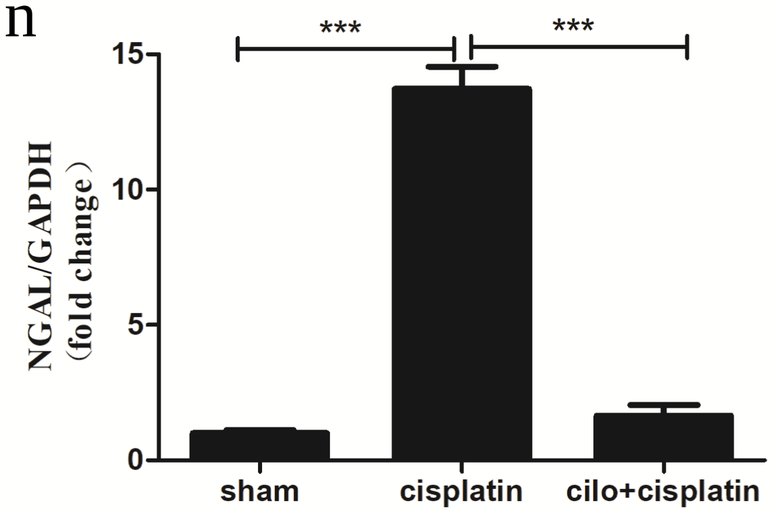

Figure 3

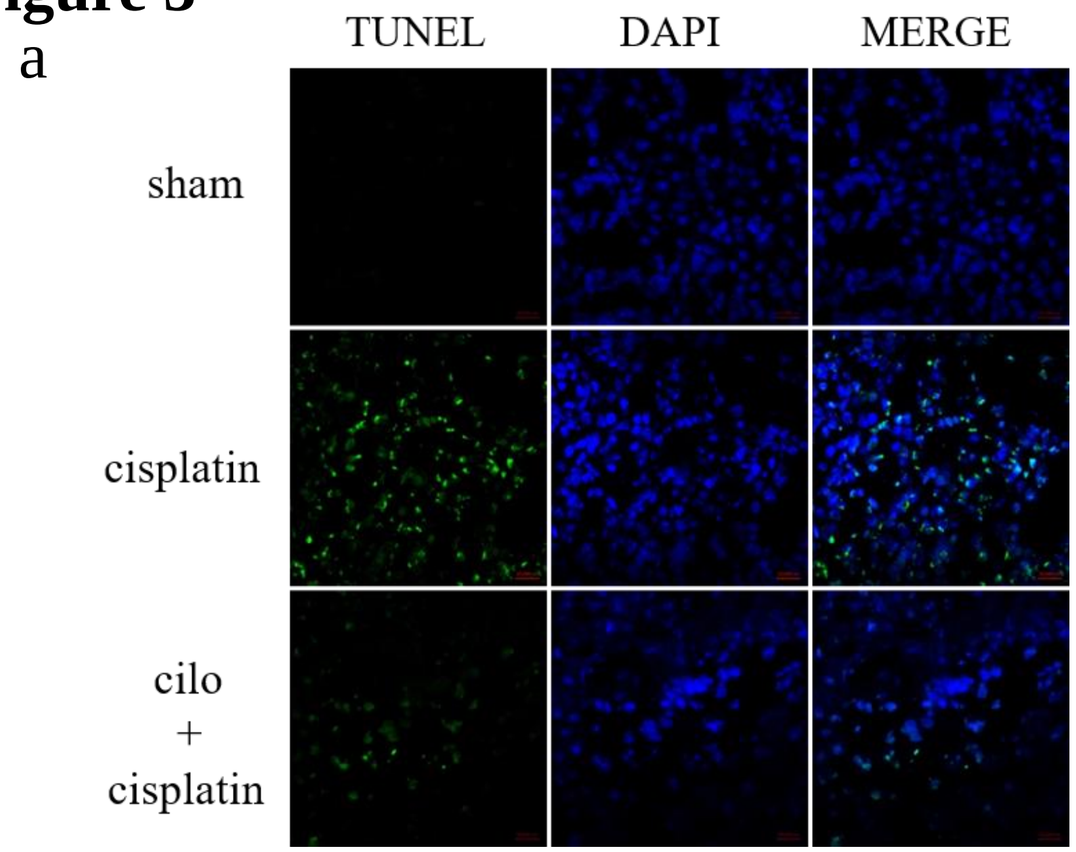

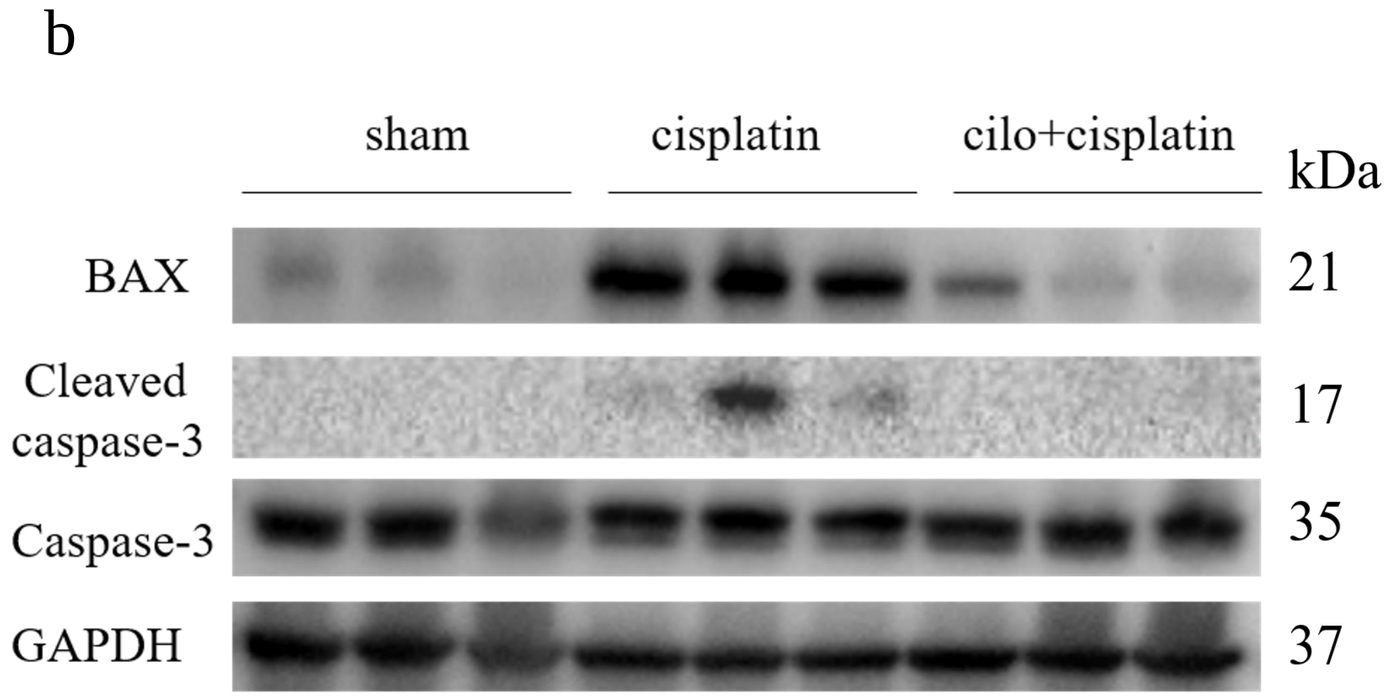

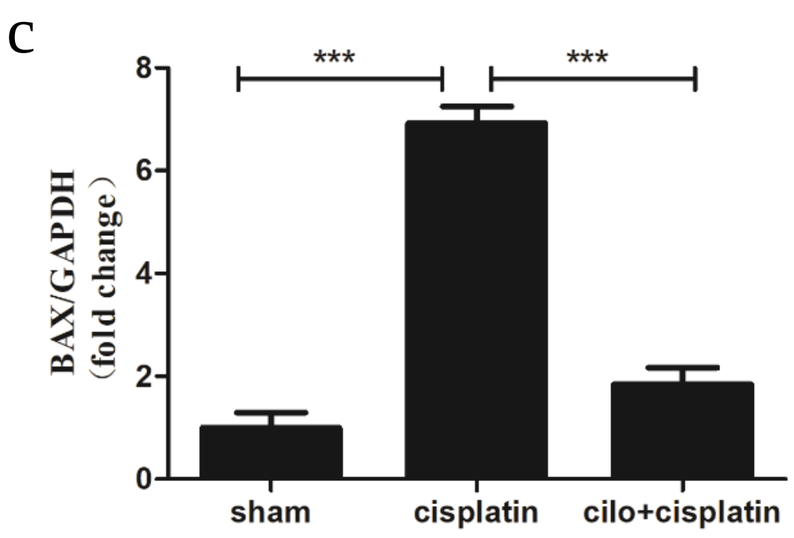

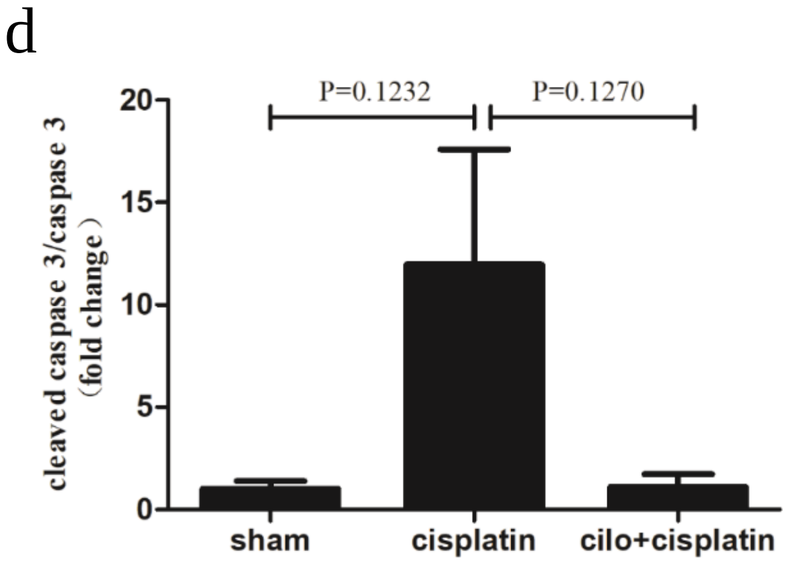

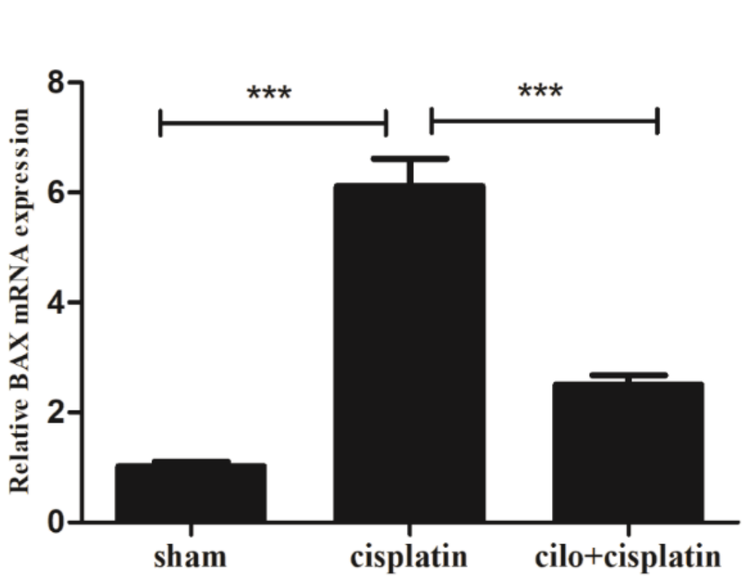

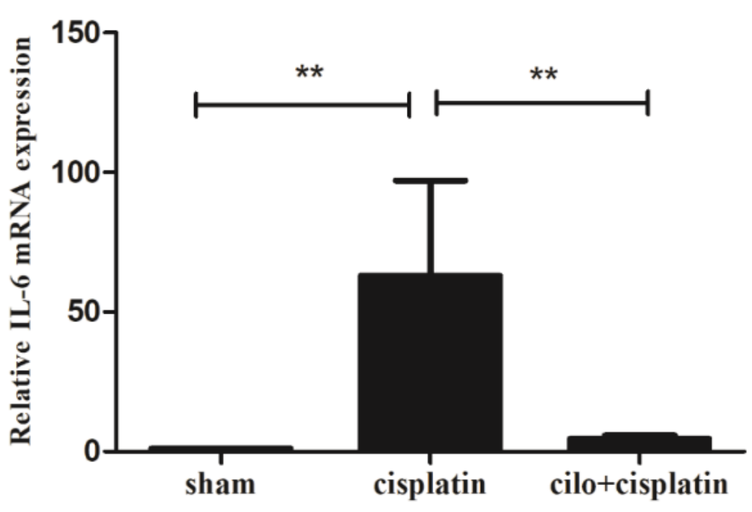

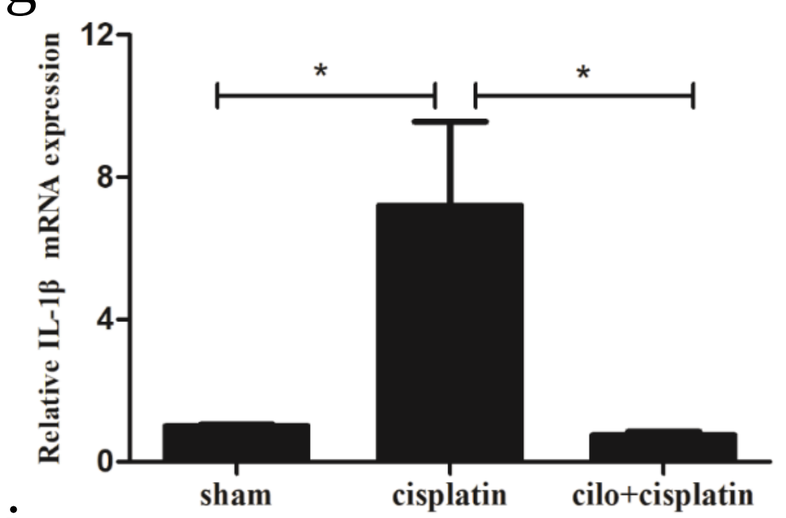

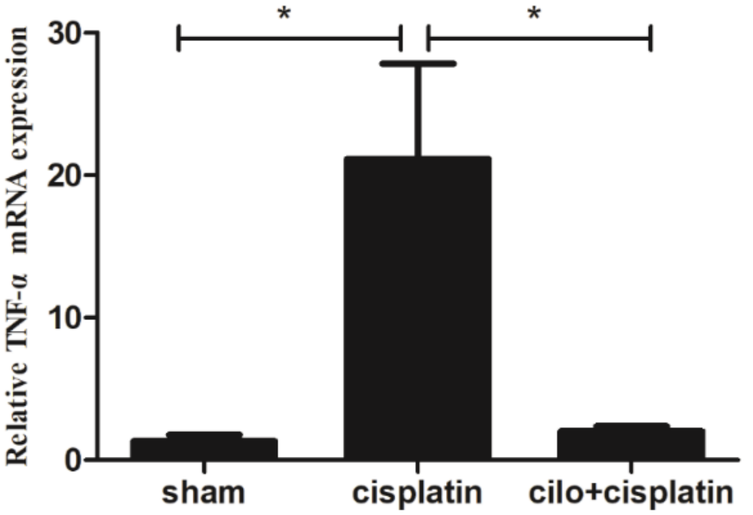

Figure 4

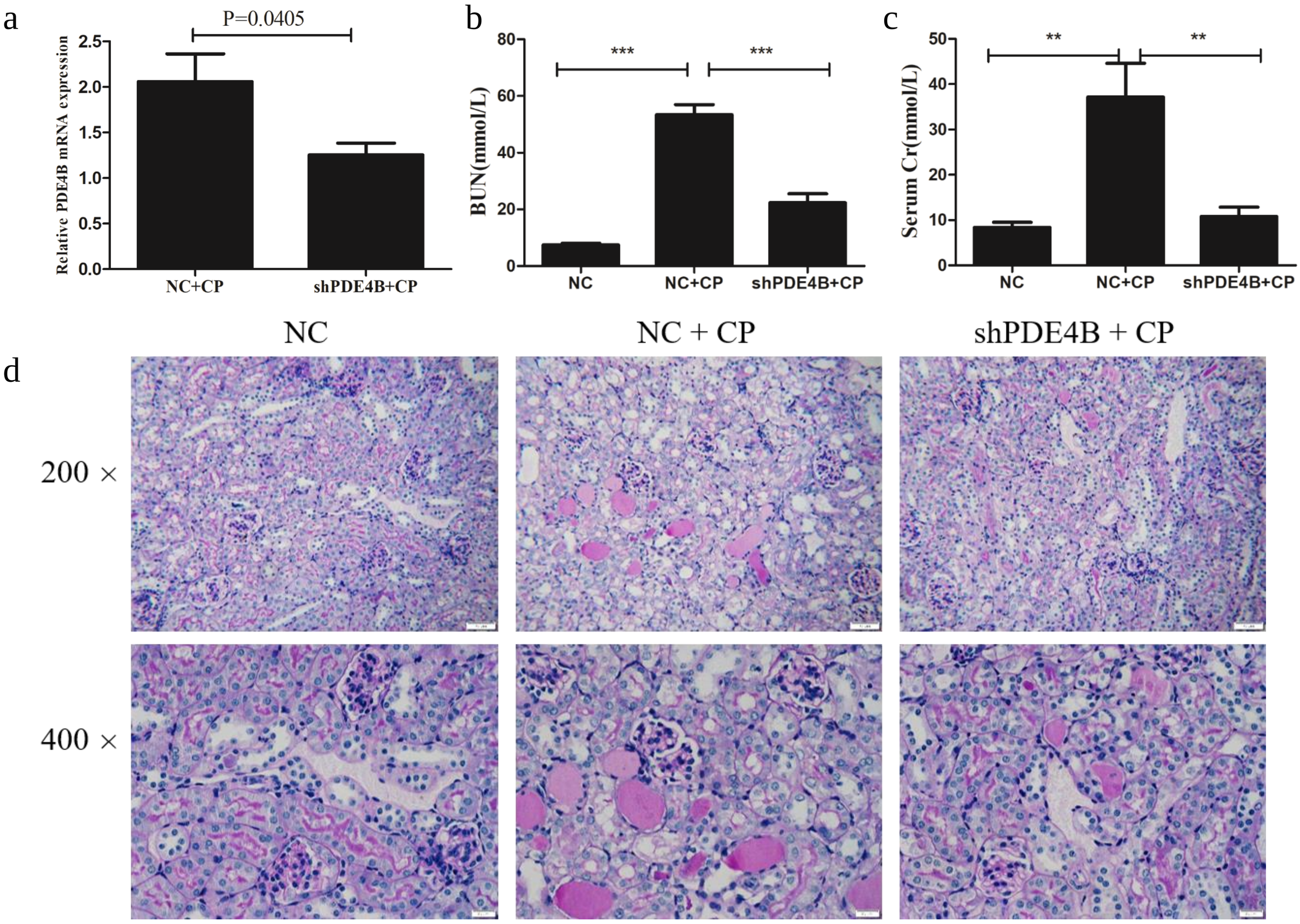

e

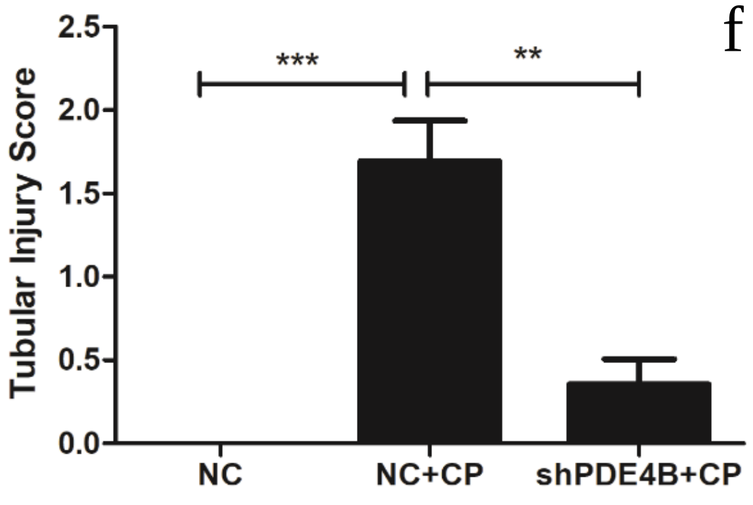

f

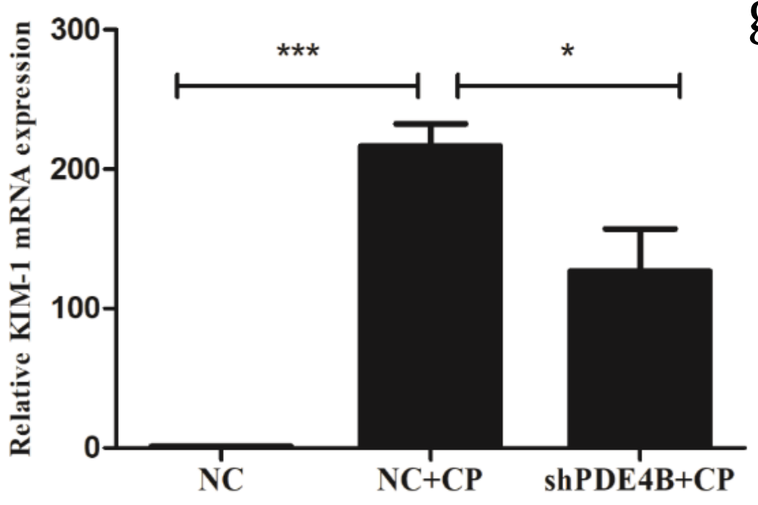

g

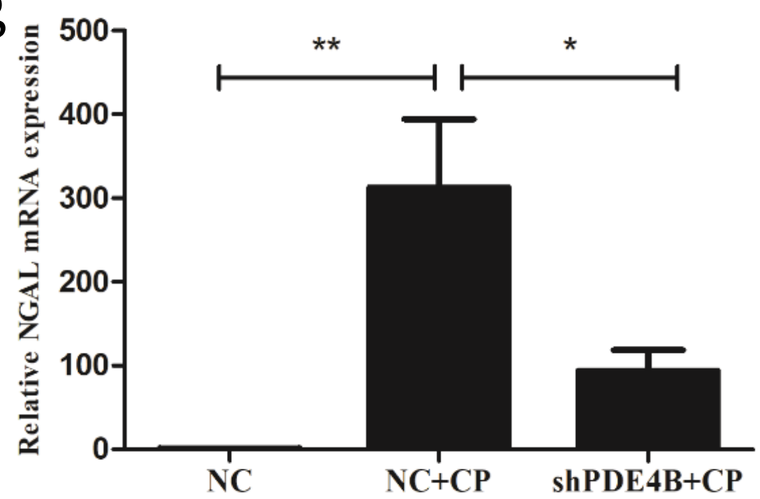

h

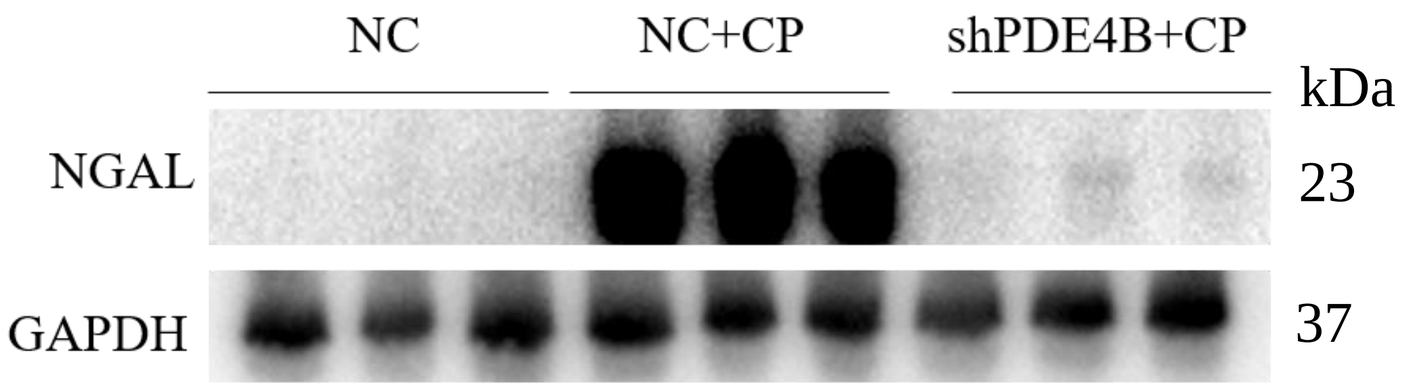

i

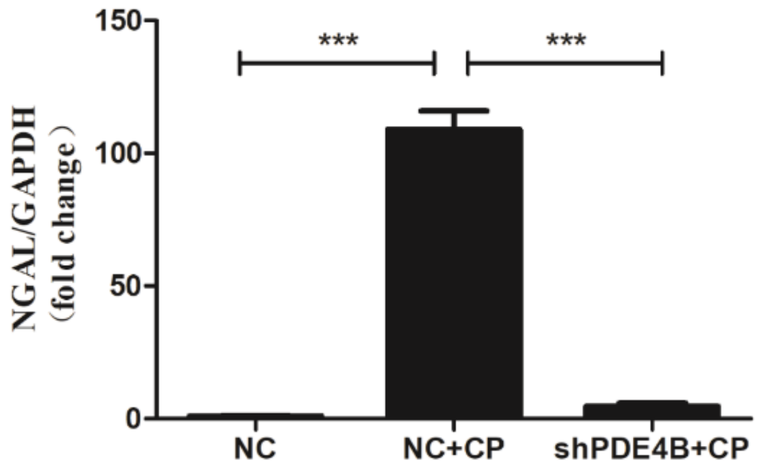

Figure 5

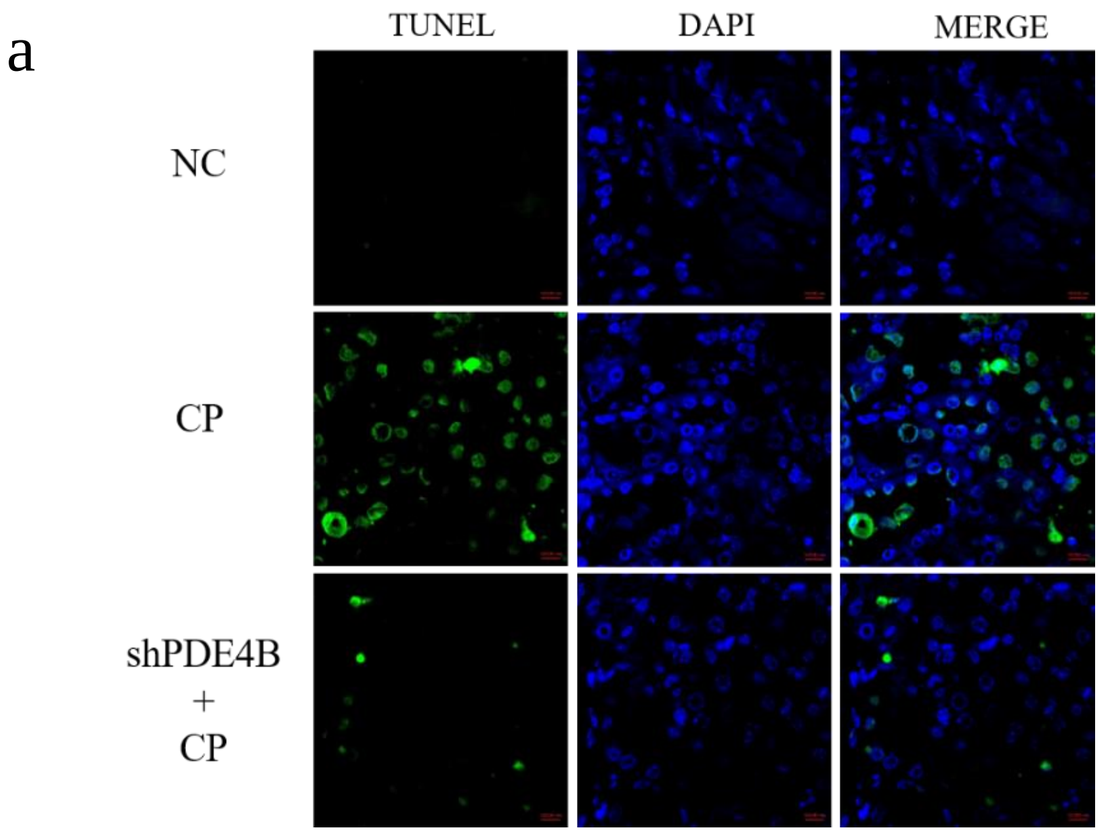

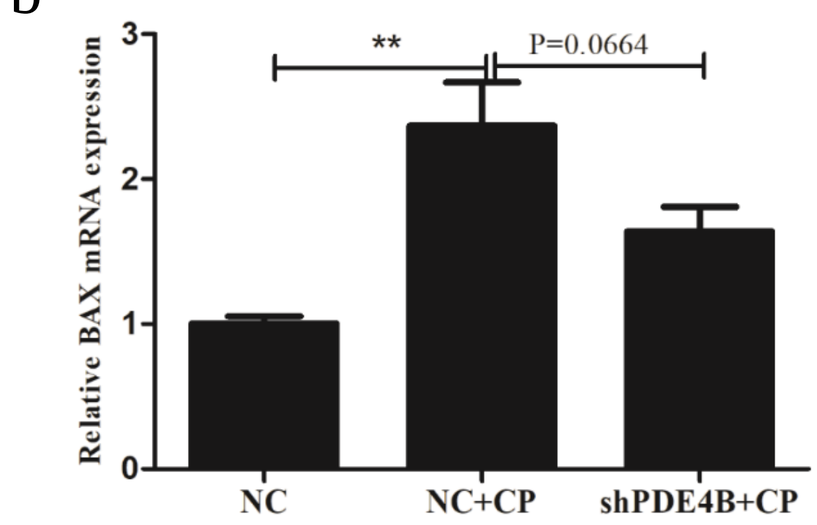

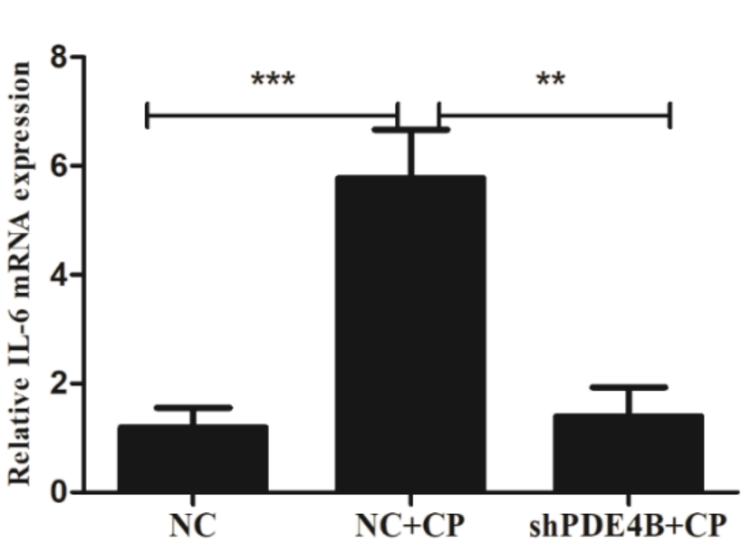

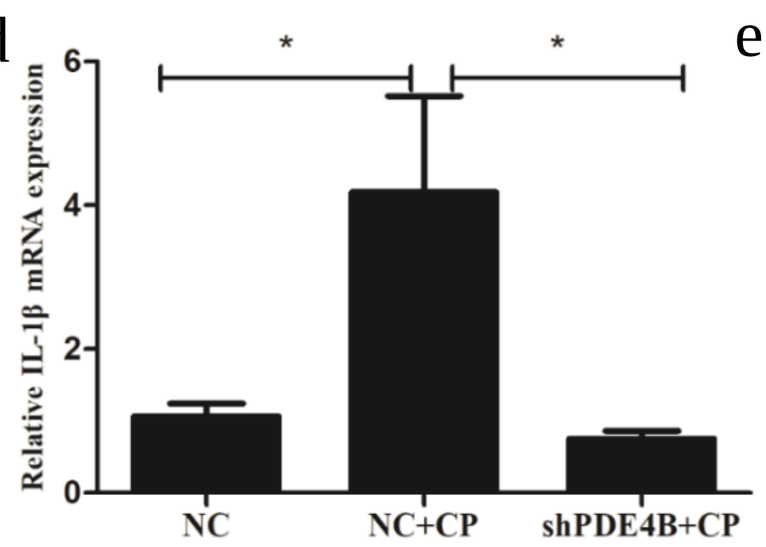

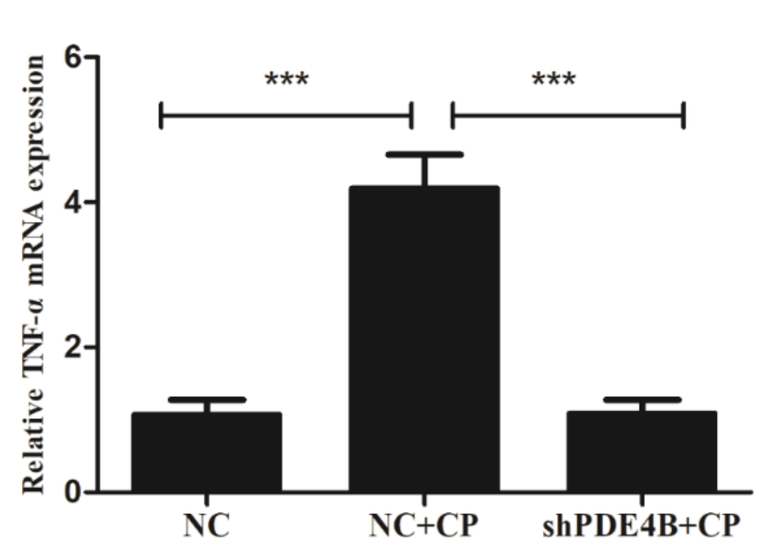

Figure 6

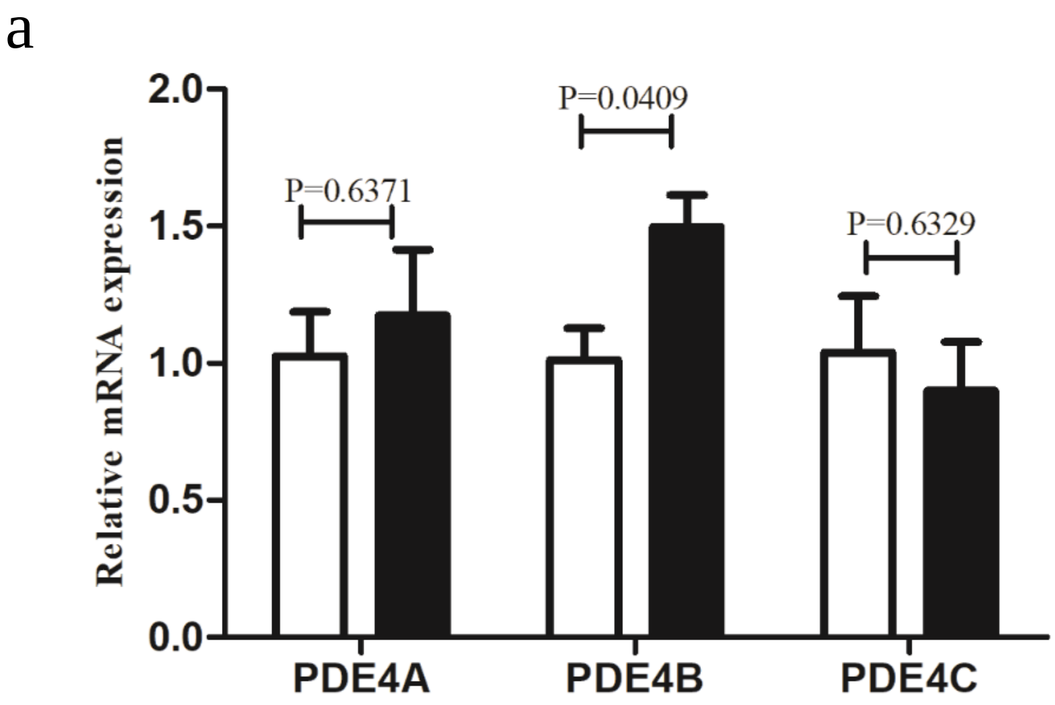

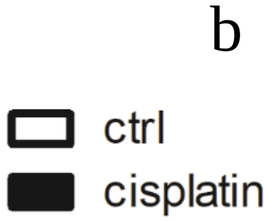

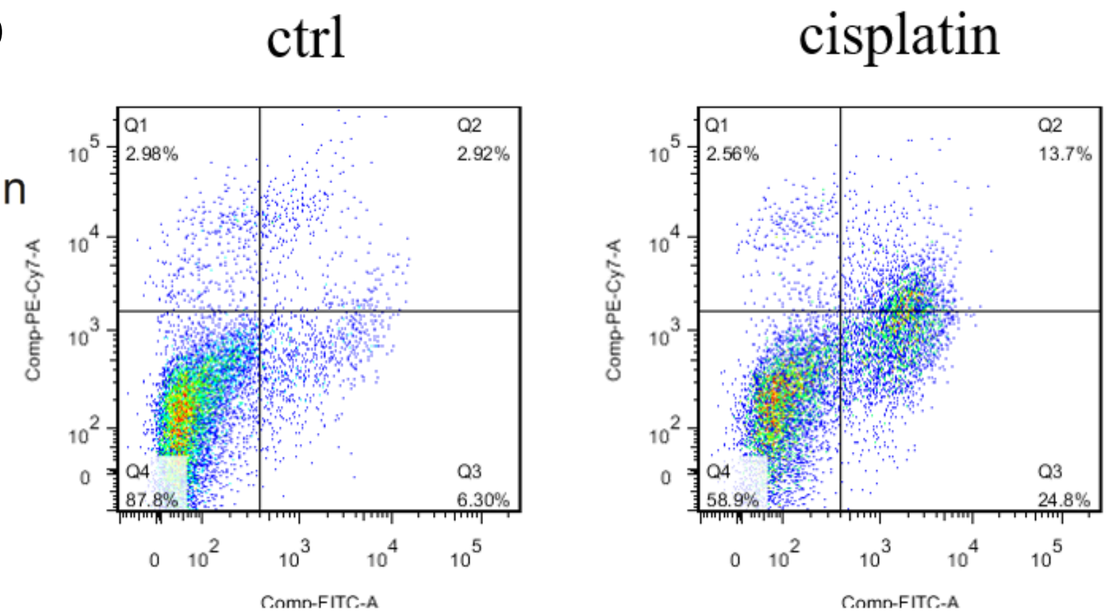

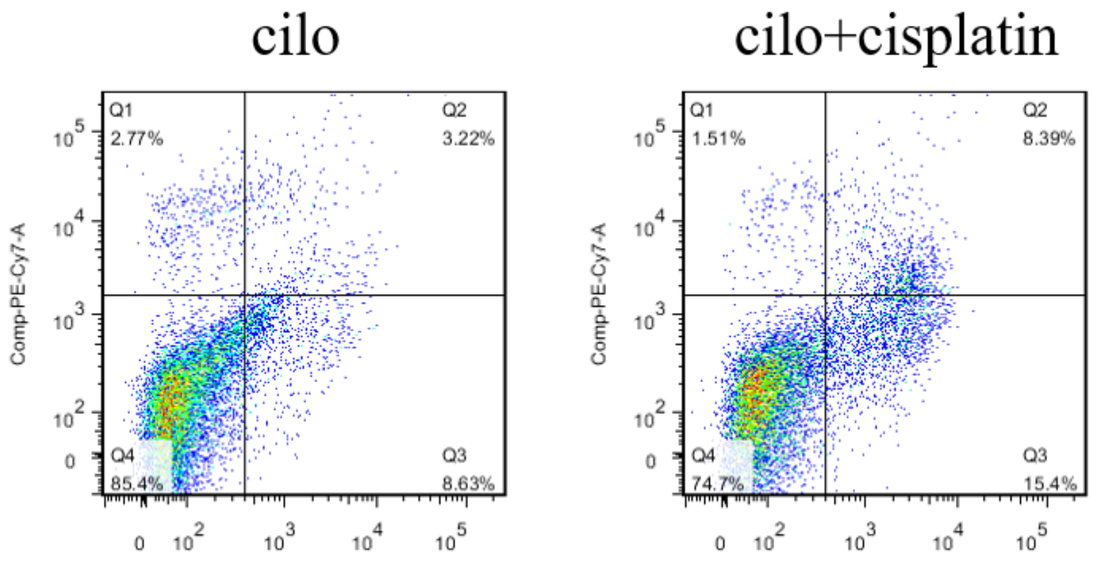

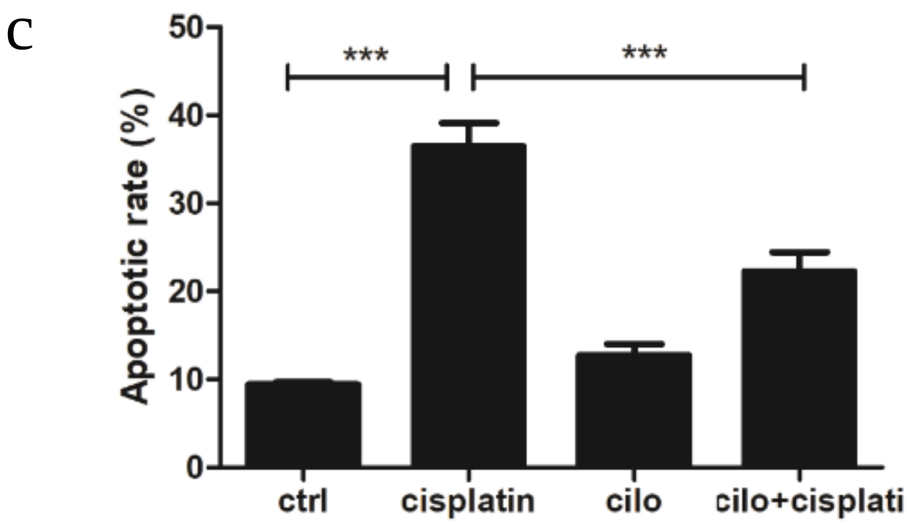

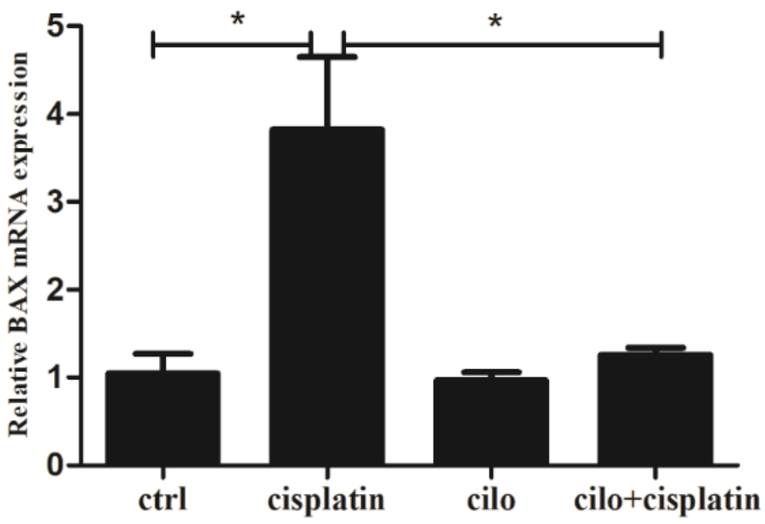

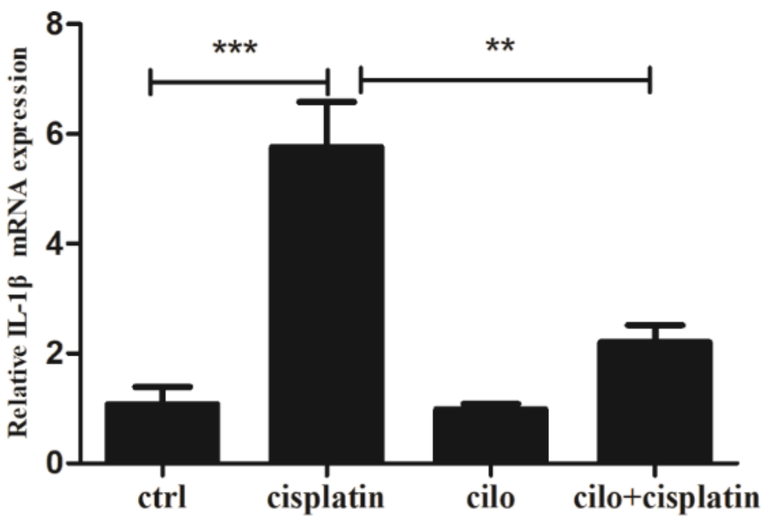

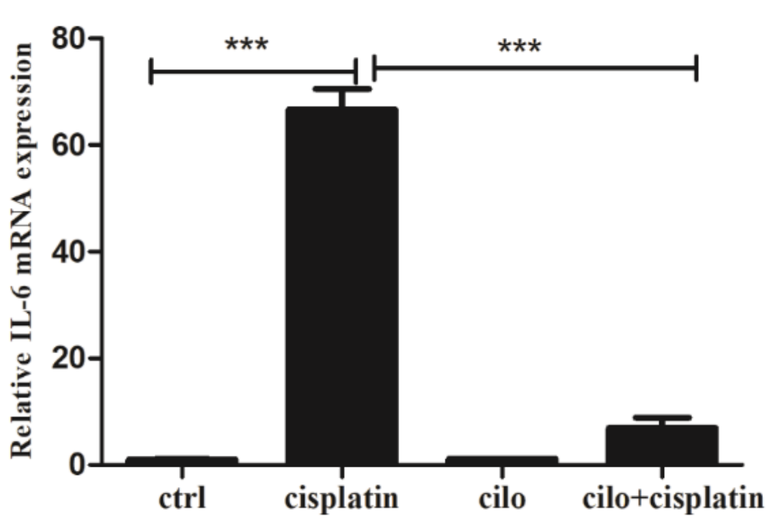

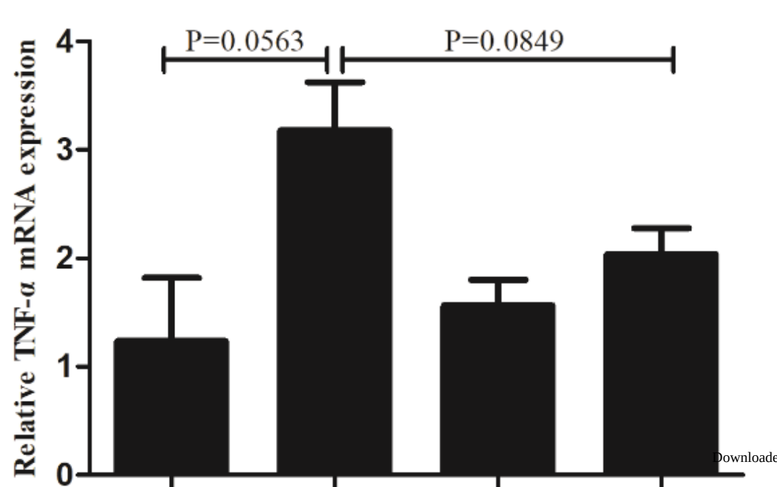

Figure 7

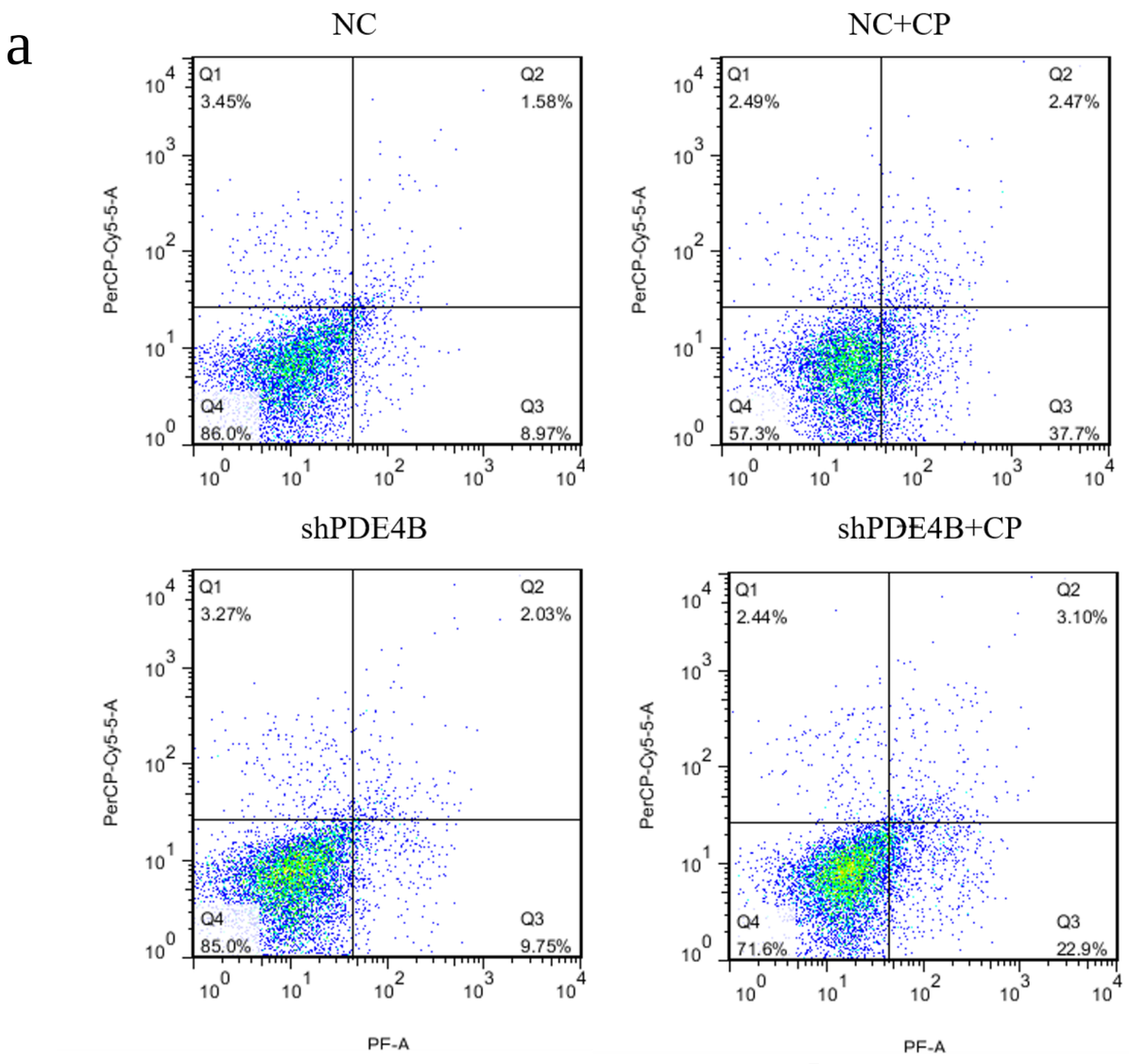

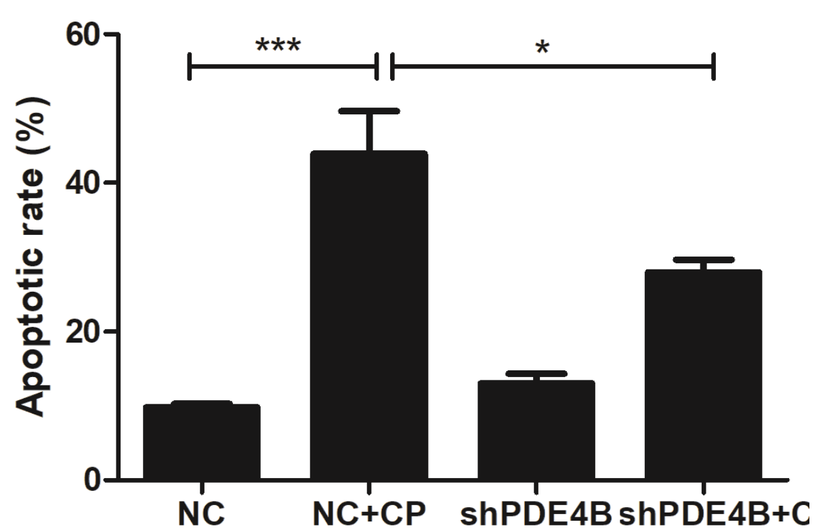

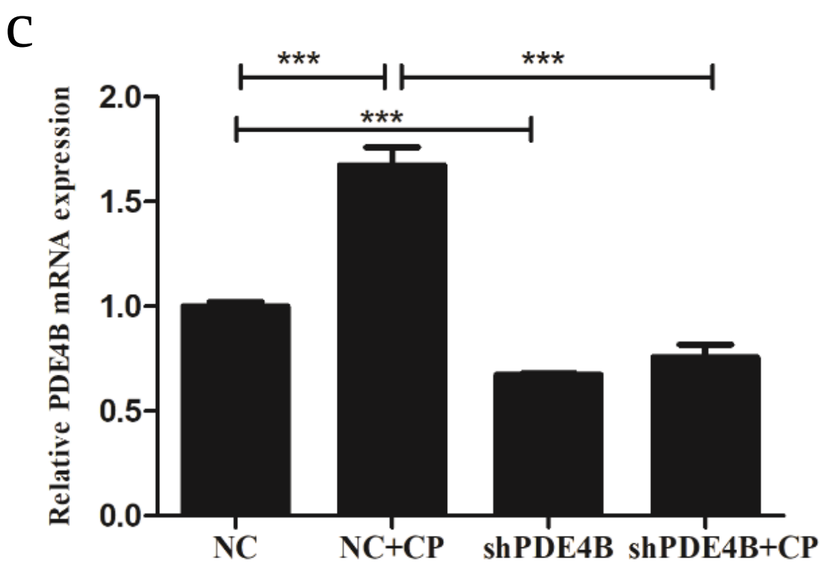

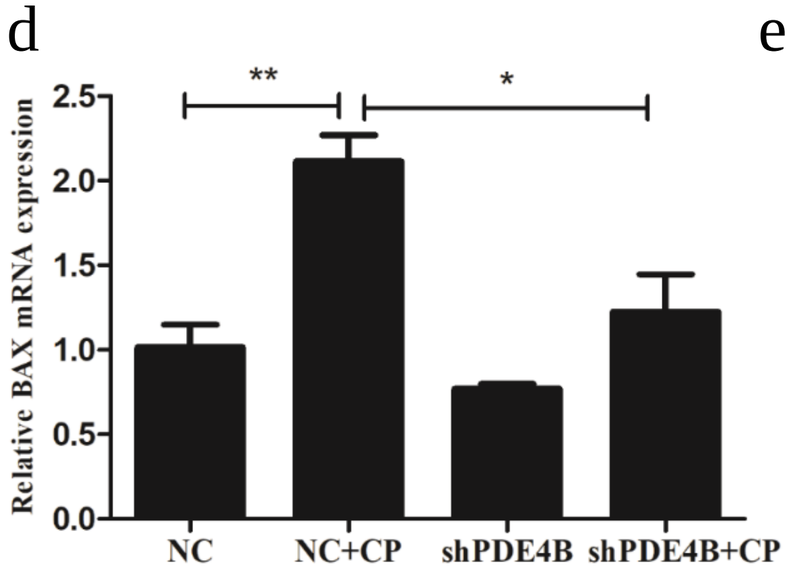

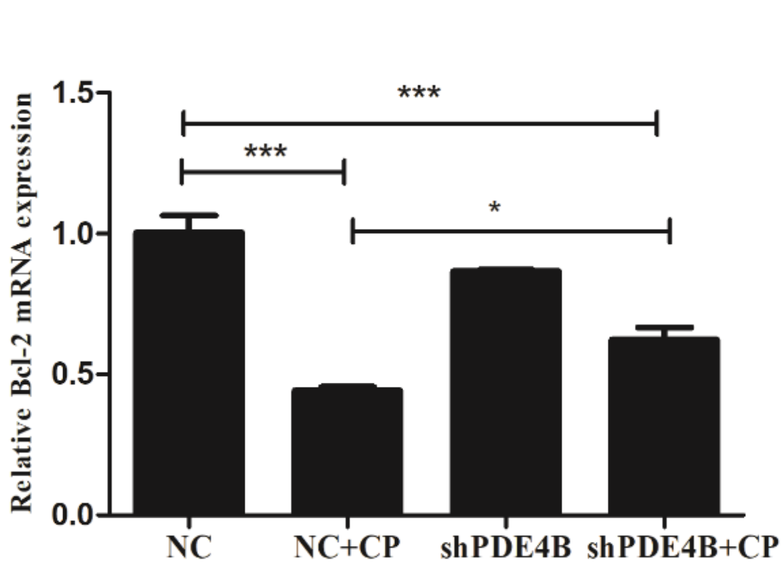

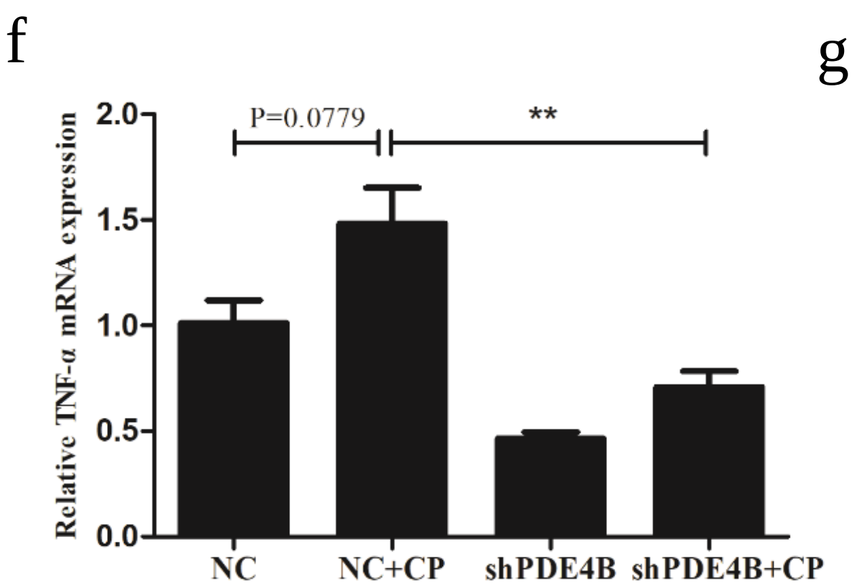

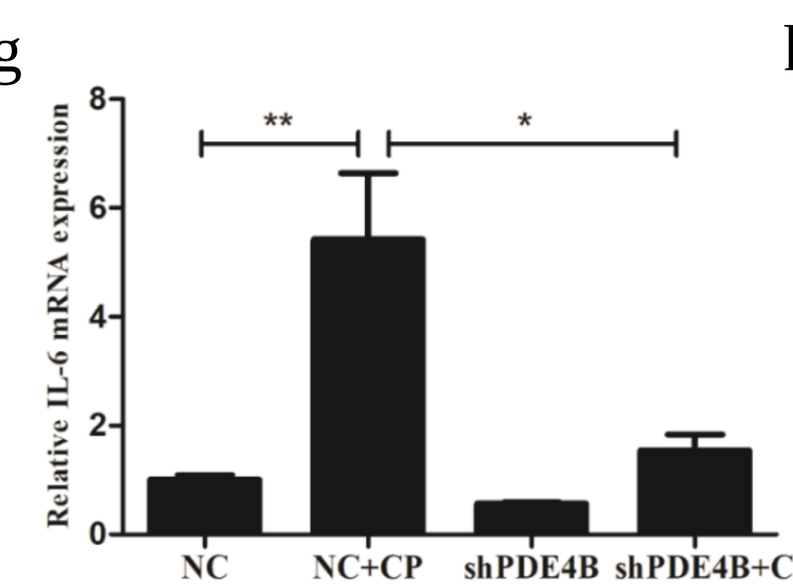

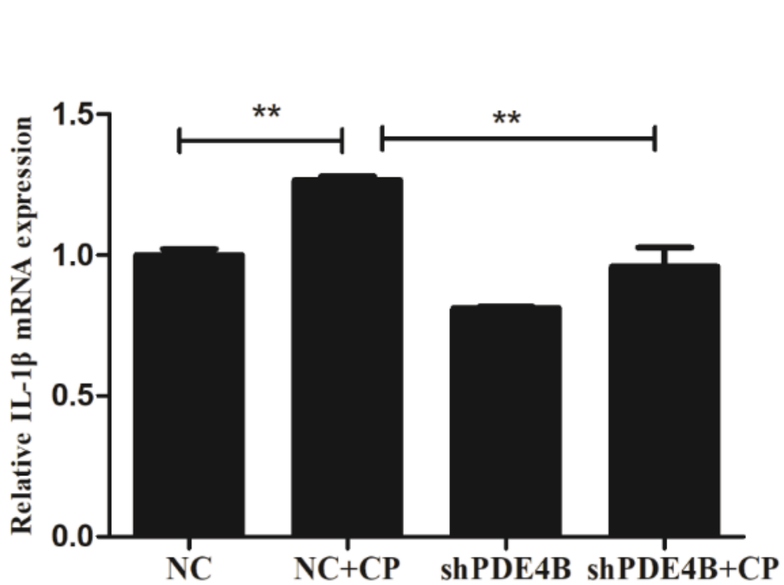

Figure 8